© 2015. Published by The Company of Biologists Ltd | Development (2015) 142, 1767-1776 doi:10.1242/dev.113894

RESEARCH ARTICLE

STEM CELLS AND REGENERATION

Glypican4 promotes cardiac specification and differentiation by attenuating canonical Wnt and Bmp signaling

Ina Strate[1], Federico Tessadori[1] and Jeroen Bakkers[1,2,*]

ABSTRACT

Glypicans are heparan sulphate proteoglycans (HSPGs) attached to the cell membrane by a glycosylphosphatidylinositol (GPI) anchor, and interact with various extracellular growth factors and receptors. The *Drosophila division abnormal delayed* (*dally*) was the first glypican loss-of-function mutant described that displays disrupted cell divisions in the eye and morphological defects in the wing. In human, as in most vertebrates, six glypican-encoding genes have been identified (*GPC1-6*), and mutations in several glypican genes cause multiple malformations including congenital heart defects. To understand better the role of glypicans during heart development, we studied the zebrafish *knypek* mutant, which is deficient for Gpc4. Our results demonstrate that *knypek*/*gpc4* mutant embryos display severe cardiac defects, most apparent by a strong reduction in cardiomyocyte numbers. Cell-tracing experiments, using photoconvertable fluorescent proteins and genetic labeling, demonstrate that Gpc4 'Knypek' is required for specification of cardiac progenitor cells and their differentiation into cardiomyocytes. Mechanistically, we show that Bmp signaling is enhanced in the anterior lateral plate mesoderm of *knypek*/*gpc4* mutants and that genetic inhibition of Bmp signaling rescues the cardiomyocyte differentiation defect observed in *knypek*/*gpc4* embryos. In addition, canonical Wnt signaling is upregulated in *knypek*/*gpc4* embryos, and inhibiting canonical Wnt signaling in *knypek*/*gpc4* embryos by overexpression of the Wnt inhibitor Dkk1 restores normal cardiomyocyte numbers. Therefore, we conclude that Gpc4 is required to attenuate both canonical Wnt and Bmp signaling in the anterior lateral plate mesoderm to allow cardiac progenitor cells to specify and differentiate into cardiomyocytes. This provides a possible explanation for how congenital heart defects arise in glypican-deficient patients.

KEY WORDS: Second heart field, Wnt signaling, Bmp signaling

INTRODUCTION

Heparan sulphate proteoglycans (HSPGs) such as glypican can interact with various growth factors, including Wnt, Bmp, Fgf and Hh, and modulate their activity (Fico et al., 2011). In most vertebrate genomes, six GPC-encoding genes have been identified (*GPC1-6*). The *Drosophila* mutant *division abnormal delayed* (*dally*) was the first glypican loss-of-function mutant described that displays disrupted cell divisions in the eye and morphological defects in the wing (Nakato et al., 1995), by affecting the signaling capacity and range of Wingless (Wnt related) and Decapentaplegic (Bmp related) (Jackson et al., 1997; Tsuda et al., 1999; Lin and Perrimon, 1999). Thus far, the only described vertebrate genetic loss-of-function models for a glypican are the *Gpc3* knock-out mouse and the zebrafish (*Danio rerio*) *gpc4* mutant. Loss of murine *Gpc3* results in a variety of embryonic defects, including developmental overgrowth and congenital heart defects (Cano-Gauci et al., 1999; Ng et al., 2009). The zebrafish *knypek/glypican4* (*kny/gpc4*) model was the first *gpc4* loss-of-function model to be described, and it is characterized by a shortened anterior-posterior body axis, craniofacial abnormalities and laterality defects (Solnica-Krezel et al., 1996; Topczewski et al., 2001). Thus far, no cardiac phenotypes in *kny/gpc4* mutants have been described.

In vertebrates, the multi-chambered heart develops from different pools of cardiac progenitor cells, termed the first and second heart field (FHF and SHF, respectively) [reviewed by Hutson and Kirby (2007); Vincent and Buckingham (2010)]. The FHF refers to a group of mesodermal cells that are the first to differentiate into cardiomyocytes and that form the early linear heart tube. The SHF refers to a region of progenitor cells located in the splanchnic mesoderm that add to the arterial and venous poles of the linear heart tube, leading to growth of the heart (Mjaatvedt et al., 2001; Waldo et al., 2001; Zaffran and Kelly, 2012). The SHF can be subdivided into different domains that are distinguished by gene expression and by their contribution to the heart [reviewed by Vincent and Buckingham (2010); Kelly (2012)]. The anterior part of the SHF expresses *Fgf8*, *Fgf10* (Kelly et al., 2001) and *Tbx1* (Xu et al., 2004) and contributes cardiomyocytes to the arterial pole of the heart. Defects in proliferation, migration or differentiation of cells from the anterior SHF result in severe congenital outflow tract defects (Goddeeris et al., 2007). The posterior SHF expresses *Hoxb1*, *Hoxa1*, *Hoxa3* and *Wnt2* (Vincent and Buckingham, 2010; Bertrand et al., 2011). Anterior and posterior SHF cells express *Islet1* (*Isl1*) and *Nkx2.5* (Vincent and Buckingham, 2010; Cai et al., 2003; Galli et al., 2008).

In zebrafish, cardiac progenitor cells are specified as two bilateral populations in the anterior lateral plate mesoderm (LPM), where they express *nkx2.5*, *hand2* and *gata4* at 12 h post fertilization (hpf) [reviewed by Bakkers (2011)]. Cell-labeling experiments in the anterior LPM at 13 to 14 hpf revealed that medially located *nkx2.5*$^{+}$*hand2*$^{+}$ progenitors predominantly form ventricle cardiomyocytes, and that the more laterally located *nkx2.5*$^{-}$*hand2*$^{+}$ progenitors predominantly form atrial cardiomyocytes (Schoenebeck et al., 2007). Consistent with these cell-labeling experiments, lineage-tracing experiments demonstrated that cardiac progenitor cells that constitute the ventricle and the OFT are specified and express *gata4* and *nkx2.5* in the anterior LPM as early as 15 hpf (Schoenebeck et al., 2007; Guner-Ataman et al., 2013). After fusion of the bilateral progenitor populations at the midline, the linear heart tube is formed around 22-24 hpf. We previously showed that the number of *myl7*-expressing cardiomyocytes in the heart tube increases rapidly from 24 to 48 hpf, whereas the rate of cardiomyocyte proliferation in the heart tube is very low (de Pater et al., 2009). Using a developmental timing assay and expression of a

[1]Department of Cardiac Development and Genetics, Hubrecht Institute & University Medical Center Utrecht, Utrecht 3584 CT, The Netherlands. [2]Department of Medical Physiology, University Medical Center Utrecht, Utrecht 3584 EA, The Netherlands.

*Author for correspondence (j.bakkers@hubrecht.eu)

Received 5 June 2014; Accepted 31 March 2015

Development (2015) 142, 1767-1776 doi:10.1242/dev.113894

photoconvertible protein, we demonstrated that the observed increase in *myl7*$^{+}$ cardiomyocytes is due to the continuous differentiation of cardiomyocytes at the poles of the heart tube, thus explaining the increase in both atrial and ventricular cardiomyocytes (de Pater et al., 2009). A distinct population of progenitor cells that express *nkx2.5*, *mef2c* and latent *TGF-β-binding protein 3* (*ltbp3*) is located anterior to the arterial pole of the linear heart tube (Lazic and Scott, 2011; Zhou et al., 2011; Hinits et al., 2012). Moreover, lineage tracing of *ltbp3*-expressing cells demonstrated that these progenitors give rise to three cardiovascular lineages (myocardium, endocardium and smooth muscle cells) at the arterial pole (Zhou et al., 2011). Thus far, it remains unclear from which progenitor population the cardiomyocytes accreted to the venous pole of the zebrafish heart are derived. Despite growing evidence that the various parts of the zebrafish heart tube are formed by distinct progenitor populations located in the anterior LPM, there is no clear definition of FHF and SHF, due to a lack of markers that could specifically label these populations. Nevertheless, several signaling pathways (e.g. FGF, Hh and TGF-β) have been identified that regulate the late differentiation of progenitors at the arterial pole in zebrafish (de Pater et al., 2009, 2012; Hami et al., 2011; Zhou et al., 2011).

Defects in human genes encoding for several members of the glypican protein family have been linked to syndromes that include congenital heart defects. Congenital heart defects are common in Simpson–Golabi–Behmel syndrome (SGBS), an X-linked syndrome caused by mutations in *GPC3* or a duplication of *GPC4* (Lin et al., 1999; Waterson et al., 2010; Fico et al., 2011). Congenital heart defects have been reported in patients with autosomal-recessive omodysplasia, which is caused by mutations in *GPC6*. A recent whole-genome association study identified a single nucleotide polymorphism in the *GPC5* gene located on chromosome 13q that was associated with Tetralogy of Fallot (TOF), a severe congenital heart defect (Cordell et al., 2013). Several individual cases with 13q deletions that include the *GPC5* gene have been reported in patients with TOF (Quelin et al., 2009).

To investigate the role of glypicans during heart development we studied the zebrafish *kny/gpc4* mutant. Whereas cardiac tissue is formed in *kny/gpc4* mutants, both the atrium and the ventricle are reduced in size. We found that the reduction in chamber size is due to compromised specification and differentiation of cardiomyocytes. Mechanistically, we found that both canonical Wnt and Bmp signaling pathways are overactivated in *kny/gpc4* mutants. Whereas inhibiting Bmp signaling in *kny/gpc4* mutants restored cardiomyocyte differentiation, overexpression of the Wnt antagonist Dkk1 restored both cardiomyocyte specification and differentiation in *kny/gpc4* mutants. Thus, our results provide a new role for Glypican4 as a regulator of canonical Wnt and Bmp signaling during cardiac differentiation. Furthermore, our study gives a potential explanation for how congenital heart defects in glypican-deficient patients can occur.

RESULTS

Loss of *knypek*/*glypican4* results in reduced cardiomyocyte numbers

In *kny/gpc4* mutant embryos, the embryonic anterior-posterior axis is reduced and they develop cardiac edema at 2 days post fertilization (dpf) (Fig. 1A,B). To investigate heart development in *kny/gpc4* mutants we carried out *in situ* hybridizations for various myosin genes and observed reduced heart looping at 58 hpf, combined with a reduction in atrial and ventricular chamber size (supplementary material Fig. S1A-F). Atrial and ventricular markers were expressed in *kny/gpc4* mutant embryos, indicating that the cardiac chambers were specified. To determine the possible cause for the reduced cardiac chamber size in *kny/gpc4* mutants, we quantified the number of *myl7*-expressing cardiomyocytes by generating a *Tg(myl7:galFF/UAS:h2a-gfp)* line in which cardiomyocytes express a nuclear green fluorescent protein (GFP) (Fig. 1D-F). Quantification of *myl7*$^{+}$ cardiomyocyte numbers revealed significantly reduced cell numbers in both the ventricle and atrium of *kny/gpc4* mutant hearts. Mutant hearts displayed an average number of 75±6 *myl7*$^{+}$ cardiomyocytes in the atrium and 71±10 cells in the ventricle, whereas wild-type sibling hearts contained an average of 129±10 *myl7*$^{+}$ cells in the atrium and 134±14 cells in the ventricle (Fig. 1G,H). In *kny/gpc4* mutant embryos, the early gastrulation defects were rescued by injection of synthetic *gpc4* mRNA (Fig. 1C). As synthetic mRNA is rapidly degraded in the embryo, late phenotypes are more difficult to rescue by this method. Indeed, we observed that the reduction in *myl7*$^{+}$ cardiomyocyte numbers was not rescued by *gpc4* mRNA injection (Fig. 1I). This result suggests that the reduced number of

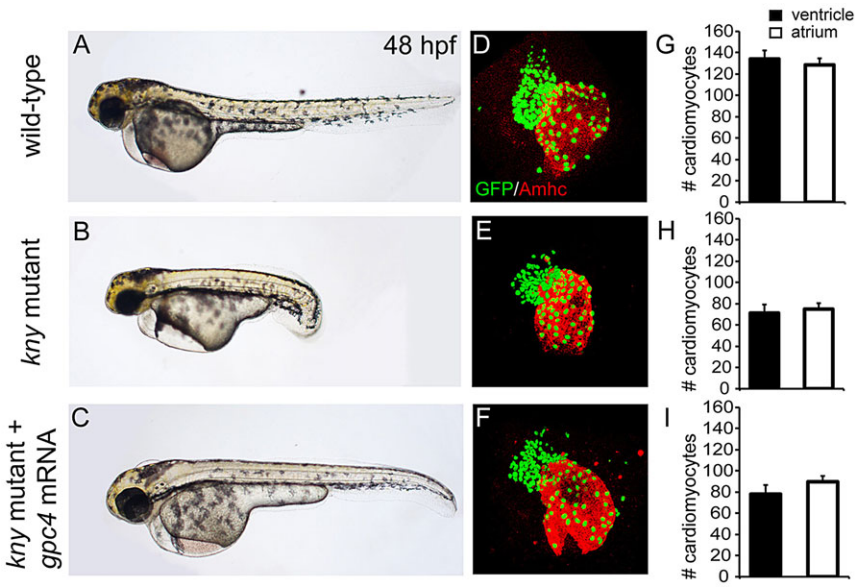

Fig. 1. Reduced cardiomyocyte numbers in *kny*/*gpc4* mutants. (A-C) Lateral view of wild type (WT) (A), *kny*/*gpc4* mutant (B) and *kny*/*gpc4* mutant injected with *kny*/*gpc4* mRNA (C) at 48 hpf. (D-F) Confocal images of hearts from *Tg(myl7:galFF/UAS:h2a-gfp, kny*$^{+/-}$*)* embryos stained for GFP and Amhc derived from WT (D), *kny*/*gpc4* mutant (E) and *kny*/*gpc4* mutant injected with *kny*/*gpc4* mRNA (F). (G-I) Quantification of number of cardiomyocytes located in either the ventricle or atrium of WT (G), *kny*/*gpc4* mutant (H) and *kny*/*gpc4* mutant injected with *kny*/*gpc4* mRNA (I) at 48 hpf (*n*=3). Results are represented as mean±s.e.m.

Development (2015) 142, 1767-1776 doi:10.1242/dev.113894

cardiomyocytes in *kny/gpc4* mutant embryos is not secondary to the gastrulation defects also observed in the mutant embryos. Together, these results demonstrate that Glypican4 is required to achieve the correct number of cardiomyocytes and normal cardiac size, and they suggest that this function is independent from its role in regulating cell movements during gastrulation.

Reduced cardiomyocyte accretion in *kny/gpc4* mutants

To determine the cause for the reduced cardiomyocyte numbers in *kny/gpc4* mutants, we first analyzed when and where *kny/gpc4* is expressed in the embryo. As previously reported, we observed a ubiquitous expression, including in the anterior LPM, where cardiac progenitors reside (supplementary material Fig. S2) (Topczewski et al., 2001). At 24-48 hpf, *kny/gpc4* expression was more restricted to the eyes, brain and pharyngeal arch region, but was absent from the heart tube. To address whether there is elevated apoptosis in the heart of *kny/gpc4* mutants, we incubated the embryos with Acridine Orange staining (supplementary material Fig. S3). We did not detect Acridine Orange^{+} cells in the hearts of *kny/gpc4* mutants, suggesting that the smaller hearts of *kny/gpc4* mutants are not caused by an elevated rate of apoptosis. Next, we investigated at which stage of development the reduction in cardiomyocyte numbers was most apparent. At 19 hpf, the cardiac field forms a disk-like epithelial structure that gives rise to the linear heart tube. We observed a moderate but significant reduction of *myl7*$^{+}$ cardiomyocytes at 19 hpf in *kny/gpc4* mutants (141±6 cells in wild type versus 123±4 cells in *kny/gpc4* mutants), consistent with a mild reduction in the expression of *nkx2.5*, *gata4* and *hand2* at 13 hpf (Fig. 2A; supplementary material Fig. S4). From 19 hpf, the linear heart tube is formed, and we previously showed that cardiomyocyte numbers increase rapidly due to the accretion of *myl7*$^{+}$ cells to the arterial and venous poles (de Pater et al., 2009). Interestingly, we observed a fourfold reduction in the accretion of *myl7*$^{+}$ cardiomyocytes in *kny/gpc4* mutants compared with their wild-type siblings (Fig. 2A). We observed an increase of 144±3 *myl7*$^{+}$ cardiomyocytes in wild-type embryos between 19 and 48 hpf, whereas the observed increase in *myl7*$^{+}$ cells was only 31±11 in *kny/gpc4* mutants. Next, we analyzed whether the accretion of *myl7*$^{+}$ cells is affected at both the venous and arterial pole by photoconversion of a fluorescent protein (Kaede or nlsKikGR) expressed in *myl7*$^{+}$ cardiomyocytes (de Pater et al., 2009; Lazic and Scott, 2011). Using *tg(myl7:gal4;UAS:Kaede)* or *tg(myl7:KikGr)* embryos, *myl7*$^{+}$ cardiomyocytes at a specific stage can be visualized by photoconversion of the fluorescent protein from green to red. Due to the continuous expression of the fluorescent protein in myl7-expressing cardiomyocytes, both the green and the photoconverted red fluorescent proteins are observed. Cardiomyocytes that initiate *myl7* expression after the photoconversion event only have the green fluorescent protein. We observed that when the Kaede photoconversion was performed at the linear heart tube stage (24-26 hpf) and analyzed at 48 hpf, green-only cardiomyocytes were detected in both the arterial pole and the venous pole of the wild-type looped heart (Fig. 2B). Interestingly, in *kny/gpc4* mutant hearts the regions of green-only myocardium at both the arterial and venous poles are reduced (Fig. 2C). To quantify the number of green-only cells, we repeated the experiment with the nuclear KikGr and observed a nearly threefold reduction in the number of green-only cardiomyocytes at the arterial pole (Fig. 2D). The weakness of the KikGr expression at the venous pole allowed only a qualitative observation (Fig. 2C). Together, these results demonstrate that Glypican4 is required for growth of the heart tube by regulating the accretion of *myl7*-expressing cardiomyocytes to both the venous and arterial poles.

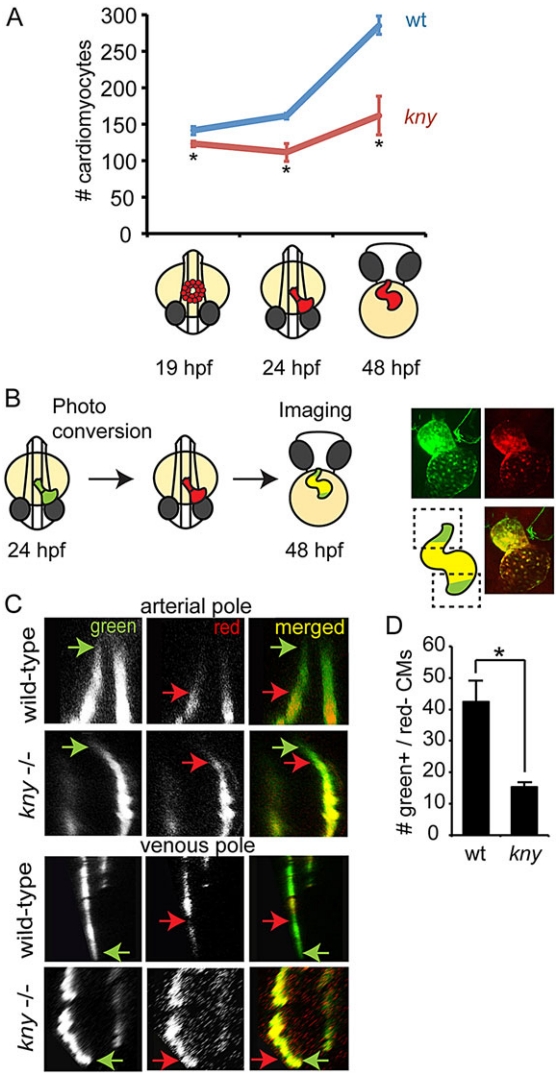

Fig. 2. Reduced cardiomyocyte accretion in *kny/gpc4* mutants. (A) Graphical representation of total cardiomyocyte counts in wild-type (wt) siblings and *kny/gpc4* mutants (*kny*) at depicted stages. (B) Schematic of photoconversion experiment, carried out at 24 hpf on *Tg(myl7:nlsKikGr)* or *Tg(myl7:galFF;UAS:Kaede)* embryos and imaged at 48 hpf to visualize non-photoconverted protein (green) and photoconverted protein (red). Boxed areas indicate regions at arterial (top) and venous (bottom) poles that were imaged to analyze the accretion of cardiomyocytes (green only). (C) Optical section at the boxed areas indicated in B at the arterial or venous pole of photoconverted *Tg(myl7:galFF;UAS:Kaede)* wild-type siblings and *kny/gpc4* mutants. Arrows in corresponding colors indicate the border of the green or the red signal, respectively. (D) Quantification of the amount of green^{+}/red^{-} cardiomyocytes that were accreted to the arterial pole between 24 and 48 hpf (n=3). *Tg(myl7:nlsKikGr)* was used for quantification. Results are represented as mean±s.e.m. *$P\leq0.05$.

Knypek/Glypican4 regulates the *nkx2.5*$^{+}$ progenitor pool and their differentiation towards *myl7*$^{+}$ cardiomyocytes

Previous work by various research groups has demonstrated that cells which are located in a region posterior to the arterial pole and express *nkx2.5*, *ltbp3* and *mef2cb* contribute to cardiac cells of the arterial pole (Lazic and Scott, 2011; Zhou et al., 2011; Hinits et al., 2012). We therefore analyzed the expression of these genes and found that they are still expressed in *kny/gpc4* mutant embryos

Development (2015) 142, 1767-1776 doi:10.1242/dev.113894

(supplementary material Fig. S5). To visualize cardiac progenitor cells in living embryos, we generated a *Tg(nkx2.5BAC:galFF/ UAS:h2a-gfp)* line in which all *nkx2.5*-expressing cells are labeled with a nuclear eGFP (further referred to as *nkx2.5:GFP*) (supplementary material Fig. S6A,B). To analyze the differentiation of progenitor cells into cardiomyocytes, we combined *Tg(myl7:dsred, kny*$^{+/-}$*)* and *Tg(nkx2.5BAC:galFF/UAS:h2a-gfp, kny*$^{+/-}$*)*, resulting in cardiomyocytes that are labeled in green (*nkx2.5:GFP*) and red (*myl7:dsred*) in the ventricle of 48-hpf embryos (Fig. 3A,B). To distinguish cardiomyocytes located in the ventricle from those in the atrium, an antibody recognizing an atrial myosin was used. We observed that at 48 hpf, the number of both *nkx2.5*$^{+}$ and *myl7*$^{+}$ cells were decreased in *kny/gpc 4* mutants (88±9 *nkx2.5*$^{+}$ cells and 64±13 *myl7*$^{+}$ cells versus 126±10 *nkx2.5*$^{+}$ cells and 135±6 *myl7*$^{+}$ cells in wild-type siblings, respectively; Fig. 3C). This is consistent with the reduced *nkx2.5* expression in *kny/gpc4* mutants at 13 hpf (supplementary material Fig. S4) and suggests that Glypican4 is required for the efficient specification and/or proliferation of cardiac progenitor cells. In addition, we observed that whereas in wild-type embryos the number of GFP^{+} to DsRed^{+} cells was almost equal (ratio of 0.93±0.06), this ratio was significantly increased to 1.4±0.13 in *kny/gpc4* mutants (Fig. 3D). *nkx2.5*$^{+}$ cells in the ventricle that fail to differentiate and initiate *myl7* expression might explain this increase in GFP^{+}/DsRed^{+}. Indeed, in ventricles of *kny/gpc4* mutants, we observed clusters of cells that expressed *nkx2.5:GFP* and not *myl7:dsred*, and these GFP-only clusters were surrounded by GFP/DsRed double-labeled cells (Fig. 3E-E″,F-F″). Such *nkx2.5:GFP*-only cells surrounded by GFP/DsRed double-labeled cells were only sparsely observed in the ventricle of wild-type siblings. Corroborating a model in which cardiomyocyte differentiation of *nkx2.5*$^{+}$ cells is compromised in *kny/gpc4* mutants, quantitative RT-PCR revealed a strong downregulation of *myl7* expression, whereas only a modest downregulation of *nkx2.5* expression was observed in *kny/gpc4* mutants at the heart-looping stage (supplementary material Fig. S6D). From these results we conclude that Glypican4 is required for efficient specification/proliferation of *nkx2.5*$^{+}$ progenitor cells and their differentiation into *myl7*$^{+}$ cardiomyocytes.

Elevated BMP signaling in *kny/gpc4* mutants compromises cardiomyocyte differentiation

To address the molecular mechanism by which Glypican4 regulates cardiac specification and differentiation, we first investigated whether BMP activity is affected in *kny/gpc4* mutants. HSPGs such as glypicans can interact with extracellular BMP, and BMP signaling is required for the induction of *nkx2.5* expression, whereas inhibition of BMP signaling promotes the differentiation of cardiac progenitor cells (Schultheiss et al., 1997; Fujise et al., 2003; Belenkaya et al., 2004; Andrée et al., 1998; Schlange et al., 2000; Yuasa et al., 2005; Matsui et al., 2005; Taha et al., 2007; Hao et al., 2008; de Pater et al., 2012; Cai et al., 2013). We analyzed Bmp signaling activity in the LPM, using a Bmp reporter line *Tg(bre:gfp)* crossed into the *kny/gpc4* mutant. We observed specifically in mutants that individual cells within the cardiac field at 19 hpf expressed high levels of GFP, which was not seen in the cardiac field of wild-type siblings (Fig. 4A-D,H). This observation indicates that Bmp signaling is ectopically activated in the cardiac field of *kny/gpc4* mutants. In addition, we observed ectopic GFP^{+} cells in the lateral plate mesoderm (Fig. 4E′-G′).

As inhibition of Bmp signaling in cardiac progenitor cells is necessary to promote cardiomyocyte differentiation (Yuasa et al., 2005; Matsui et al., 2005; Taha et al., 2007; Hao et al., 2008; de

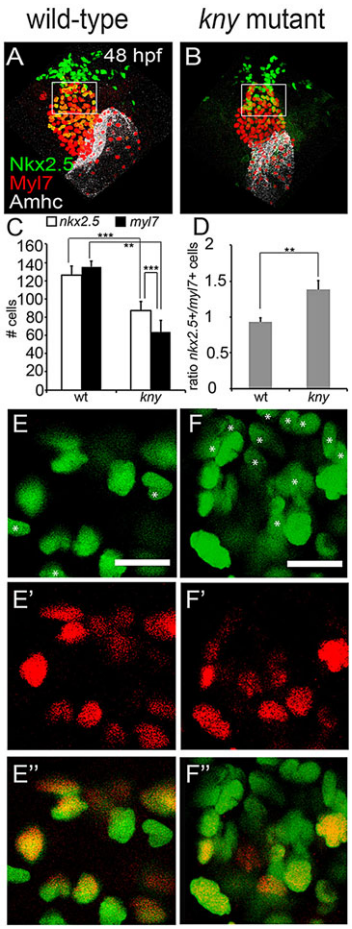

Fig. 3. Compromised cardiomyocyte differentiation in *kny/gpc4* mutants. (A,B) Embryonic hearts of wild-type and *Tg(nkx2.5BAC:galFF/UAS:h2a-gfp, myl7:dsred, kny*$^{+/-}$*)* embryos after immunohistochemistry against GFP (Nkx2.5, green), DsRed (Myl7, red) and Amhc (white) at 48 hpf. Boxed areas indicate the regions shown in higher magnification in E″,F″ and used for quantification in C,D. (C) Numbers of *nkx2.5*$^{+}$ and *myl7*$^{+}$ cells in the ventricles of wild-type siblings and *kny/gpc4* mutants (*n*=5). (D) Ratio of *nkx2.5*$^{+}$/*myl7*$^{+}$ cells in wild-type siblings and *kny/gpc4* mutants (*n*=5). (E-E″) Higher magnification views of the ventricle of a wild-type sibling, showing sparse *nkx2.5*$^{+}$-only cells (white asterisks). (F-F″) Corresponding area in a *kny/gpc4* mutant, displaying a typical cluster of *nkx2.5*$^{+}$ cells. Scale bars: 15 µm. Results are represented as mean±s.e.m. $^{**}P \leq 0.01$, $^{***}P \leq 0.001$ in paired *t*-test.

Pater et al., 2012; Cai et al., 2013), we hypothesized that elevated Bmp signaling in the anterior LPM is responsible for the reduction of cardiomyocyte numbers in *kny/gpc4* mutants. To test this hypothesis, we crossed the *Tg(hsp70:nog)*, in which the Bmp antagonist Noggin3 is induced upon heat shock, into the *kny/gpc4* mutant line. Induction of Noggin3 at 16 hpf in wild-type embryos results in a moderate reduction in atrial cardiomyocytes, whereas the number of ventricular cardiomyocytes remains unaffected, probably reflecting the temporal differences in the specification of atrial versus ventricular progenitor cells (de Pater et al., 2012). Corroborating our hypothesis, induction of Noggin3 at 16 hpf in *kny/gpc4* mutants resulted in a modest but significant increase in *myl7*$^{+}$ ventricular cardiomyocytes (Fig. 5A-C). Moreover, when combining the *Tg(hsp70:nog)* with the *Tg(nkx2.5:galFF;UAS:h2a-gfp)* and the *Tg(myl7:dsred)*, we observed that although the number of *myl7*$^{+}$ cardiomyocytes in *kny/gpc4* mutants increased, there was no effect on the number of *nkx2.5*$^{+}$ cells as a consequence of Noggin3 overexpression (Fig. 5D). As a result, Noggin3 overexpression

Development (2015) 142, 1767-1776 doi:10.1242/dev.113894

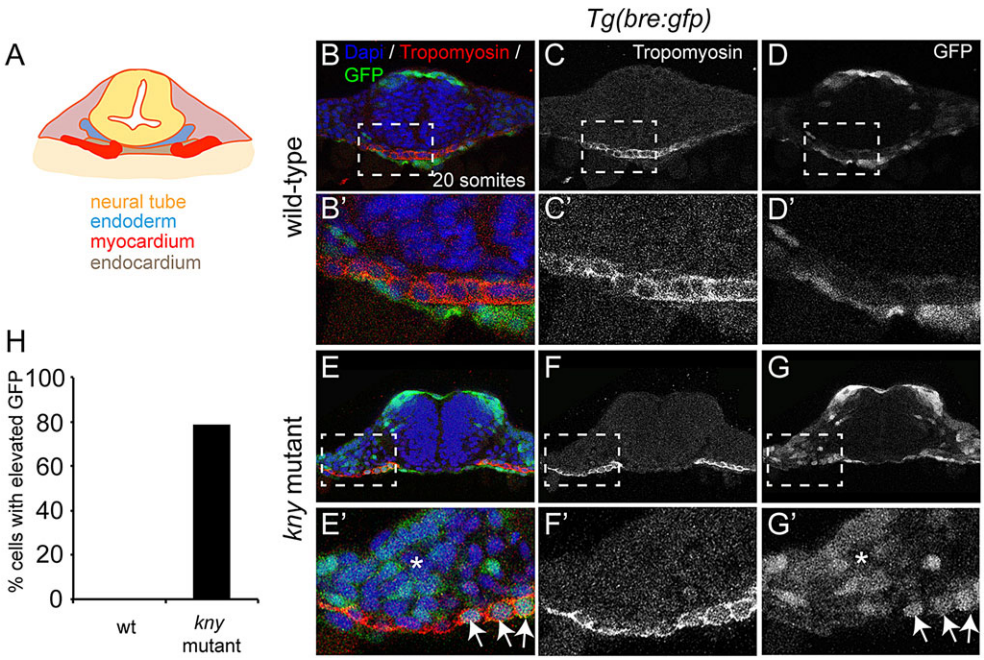

Fig. 4. Elevated Bmp signaling in *kny/gpc4* mutants. (A) Schematic cross-section through the anterior LPM of a 20-somite stage embryo. (B-G′) Cross-sections of WT (B-D′) or *kny/gpc4* mutant (E-G′) embryos with *Tg(bre:gfp)*. Cell nuclei are shown in blue (DAPI), cardiac tissue in red (tropomyosin) and Bmp activity in green (*bre:gfp* transgene). B′-D′ and E′-G′ are higher magnification views of boxed areas in B-D and E-G, respectively. Arrows indicate GFP^+ cardiomyocytes. Asterisks indicate lateral plate mesoderm with GFP^+ cells. (H) Percentage of cardiomyocytes in *kny/gpc4* mutants with higher GFP pixel intensity than the 1.5-fold average value for wild-type cardiomyocytes (n=2, 14 cells).

restored the abnormally high ratio of GFP^+/$DsRed^+$ cells in *kny/gpc4* mutants from 1.4±0.12 to 0.8±0.02 (Fig. 5E). Together, these results suggest that blockage of excessive Bmp signaling in *kny/gpc4* mutants does not affect cardiomyocyte specification but leads to a restoration of cardiomyocyte differentiation.

Inhibiting canonical Wnt signaling restores cardiomyocyte numbers in *kny/gpc4* mutants

HSPGs can also bind different Wnt ligands and the Wnt-promoting factor R-spondin, and affect both canonical as well as non-canonical Wnt signaling (Topczewski et al., 2001; Ohkawara et al., 2011; Sakane et al., 2012). To investigate whether canonical Wnt signaling in *kny/gpc4* mutants was affected, we performed *in situ* hybridizations for *axin2*, a direct target gene of canonical Wnt signaling. Interestingly, we observed an upregulation of *axin2* expression in the anterior lateral plate mesoderm of *kny/gpc4* mutants (Fig. 6A-D).

We have previously shown that Wnt signaling is upstream of BMP signaling in the heart of 48 hpf embryos (Verhoeven et al., 2011). To test whether, in *kny/gpc4* mutants, the ectopic BMP activation observed at 20 hpf could be the consequence of enhanced canonical Wnt signaling, we crossed the *Tg(hsp70:wnt8a-gfp)* line with a BMP reporter line expressing an orange fluorescent protein, *Tg(bre:dmKO2)*, and heat-shocked embryos at 16 hpf (Collery and Link, 2011). In contrast to later stages of heart development, we did not detect enhanced bre:dmKO2 activity in the cardiac disk or LPM of heat-shocked *wnt8-gfp* embryos (supplementary material Fig. S7), indicating that at 16 hpf, ectopic Wnt signaling does not induce Bmp signaling.

Canonical Wnt signaling can have both positive and negative effects on cardiac specification and differentiation, dependent on the developmental stage when being induced (Manisastry et al., 2006; Verma and Lenka, 2010; Dohn and Waxman, 2012; Willems et al., 2011). Using the heat shock-inducible Wnt8 line *Tg(hsp70:wnt8-gfp)*, we indeed observed that induction of Wnt8 at 16 hpf reduced the number of ventricular cardiomyocytes (supplementary material Fig. S8C-E). To address whether this was due to compromised cardiac specification or differentiation, we combined the *Tg(hsp70:wnt8-gfp)* with the *Tg(nkx2.5:galFF; UAS:h2a-gfp)* and the *Tg(myl7:dsred)*, and observed that both $nkx2.5^+$ cells and $myl7^+$ cells were reduced as a consequence of ectopic Wnt8 expression (supplementary material Fig. S8F). As the ratio of $nkx2.5^+/myl7^+$ cells in the ventricle was also affected by ectopic Wnt8 expression, these results indicate that both cardiomyocyte specification and differentiation are affected by ectopic canonical Wnt signaling at 16 hpf (supplementary material Fig. S8G). To test the hypothesis that in *kny/gpc4* mutants, the observed reduction in cardiomyocyte specification and differentiation is due to an upregulation of canonical Wnt signaling, we aimed to restore cardiomyocyte numbers in *kny/gpc4* mutants by blocking canonical Wnt signaling. Temporally controlled inhibition of canonical Wnt signaling was achieved using the previously described heat shock-inducible *Tg(hsp70:dkk1-gfp)* line (Stoick-Cooper et al., 2007). Corroborating our hypothesis, inhibition of canonical Wnt signaling in *kny/gpc4* mutants by overexpression of the Wnt inhibitor Dkk1 at 16 hpf resulted in a significant increase in the number of $myl7^+$ cardiomyocytes in both atrium and ventricle (Fig. 6E-G). Overexpression of Dkk1 in *kny/gpc4* mutants at 24 hpf had no effect on the number of $myl7^+$ cardiomyocytes (Fig. 6G). From these results, we conclude that Glypican4 is required to attenuate canonical Wnt signaling at 16 hpf, which is required to allow sufficient cardiomyocytes to be specified. Whereas inhibiting canonical Wnt signaling in *kny/gpc4* mutant embryos rescued cardiomyocyte numbers, cardiac morphology was still affected. Heart looping was still disturbed in *kny/gpc4* mutants after inhibition of Wnt signaling, and the atrial-ventricular canal was still broader than in wild-type siblings (Fig. 6F), indicating that Glypican4 has additional roles in cardiac development independent from canonical Wnt signaling.

DISCUSSION

Whereas defects in human genes encoding for several members of the glypican protein family have been linked to syndromes that include congenital heart defects, very little was known about their role during heart development. Our genetic and embryological analysis of Glypican4-deficient zebrafish embryos demonstrates

Development (2015) 142, 1767-1776 doi:10.1242/dev.113894

that Glypican4 is required to regulate cardiomyocyte formation in the anterior LPM. As a result of Glypican4 deficiency there are fewer *nkx2.5*$^{+}$cells in the embryonic heart and even fewer differentiated *myl7*$^{+}$ cardiomyocytes, providing an explanation for the small hearts of *kny/gpc4* mutants. Mechanistically, we propose that Glypican4 is required to attenuate both canonical Wnt and Bmp signaling in the anterior LPM and that this attenuation is required to ensure the formation of sufficient nkx2.5^{+} cardiac progenitor cells and their differentiation into cardiomyocytes (Fig. 6I). Glypicans, as other HSPGs, are decorated with long heparin chains that interact extracellularly with various secreted growth factors, including Wnt and BMP (Desbordes and Sanson, 2003; Williams et al., 2010). Such interactions can control growth factor signaling by regulating growth factor availability or facilitating interactions with (co)-receptors (see below) (Fig. 6H). Our results suggest that Glypican4 attenuates both Wnt and BMP signaling independently, possibly by preventing their release from the ECM and interaction with their receptor complex during cardiac specification and differentiation.

Here, we show that loss of Glypican4 results in a local enhancement of Bmp signaling and that inhibiting Bmp signaling in *kny/gpc4* mutants can rescue the cardiomyocyte differentiation defects by restoring the normal ratio of nkx2.5^{+} and myl7^{+} cells in the ventricle. Interestingly, inhibition of BMP signaling in *kny/gpc4* mutants did not restore the number of nkx2.5^{+} cells, suggesting that other functions of Glypican4 (e.g. attenuating Wnt signaling) regulate this process. Indeed, BMP signaling and Wnt signaling have distinct roles in regulating SHF specification and differentiation in the anterior LPM of mouse embryos (Klaus et al., 2012). Our observation that Glypican4 is required to attenuate BMP signaling to allow proper differentiation of myl7^{+} cardiomyocytes is consistent with a model in which BMP signaling is required to induce *nkx2.5* expression in the anterior LPM, but that BMP signaling in cardiac progenitor cells needs to be downregulated to allow efficient cardiomyocyte differentiation (Hao et al., 2008; de Pater et al., 2012; Cai et al., 2013). Glypicans have been implicated in the control of TGF-β/Bmp activity (Jackson et al., 1997; Paine-Saunders et al., 2000; Li et al., 2004). The *Drosophila* glypican Dally is required for the modulation of the signaling strength of the TGF-β/Bmp-superfamily member Decapentaplegic (Dpp) (Fujise et al., 2003; Belenkaya et al., 2004). It could thus be hypothesized that Glypican4 attenuates BMP signaling through physical interaction of the heparin chains with the BMP growth factor in the extracellular space, and subsequently prevents it from activating Smad protein phosphorylation in the cardiac progenitor cells.

Besides a role in attenuating BMP signaling, our results also indicate that Glypican4 is required to attenuate canonical Wnt signaling. A role for glypicans in regulating canonical Wnt signaling was shown in *Drosophila*, demonstrating that *gpc4* homolog *dally-like* is essential for Wg gradient formation (Han et al., 2005). As proposed for BMP signaling, one possible hypothesis is that Glypican4 affects the extracellular distribution of Wnt growth factors. Alternatively, Glypican4 might interact with specific components of the Wnt signaling pathway. Corroborating such a model is the observation that Glypican4 can modulate Wnt/β-catenin and Wnt/PCP signaling pathways through interactions with Dkk1 and LRP5/6 (Caneparo et al., 2007). Moreover, in more recent studies it was shown that glypicans are required for the Wnt-inhibiting activity of Wnt Inhibitory Factor-1 (WIF-1) (Avanesov et al., 2012). *In vitro*, the Wnt-promoting factor R-spondin 3 was shown to interact with Syndecans and Glypican3 (Ohkawara et al., 2011), suggesting a complex interaction of heparan sulphate proteoglycans and Wnt signaling components at the cell membrane. Interestingly, human SGBS patients have a tendency to develop pre- and postnatal tumors, such as Wilm's tumor, hepatoblastomas, neuroblastomas and gonadoblastomas (Golabi et al., 1993; Rodríguez-Criado et al., 2005; Thomas et al., 2012; Mateos et al., 2013). The development of these tumors has been brought into correlation with a misregulation of canonical Wnt signaling (Honecker et al., 2004; Lapunzina, 2005; Liu et al., 2008; Armengol et al., 2011), indicating that the lack of glypicans might result in a misregulation of canonical Wnt signaling in SGBS patients. It remains to be addressed how Glypican4 attenuates Wnt signaling in the anterior LPM during cardiac specification and differentiation.

Although we observed that cardiomyocyte numbers in *kny/gpc4* mutants were fully restored by inhibiting canonical Wnt signaling (Fig. 6G), we also observed that heart morphology was still affected in these rescued embryos (Fig. 6F). The hearts of the rescued

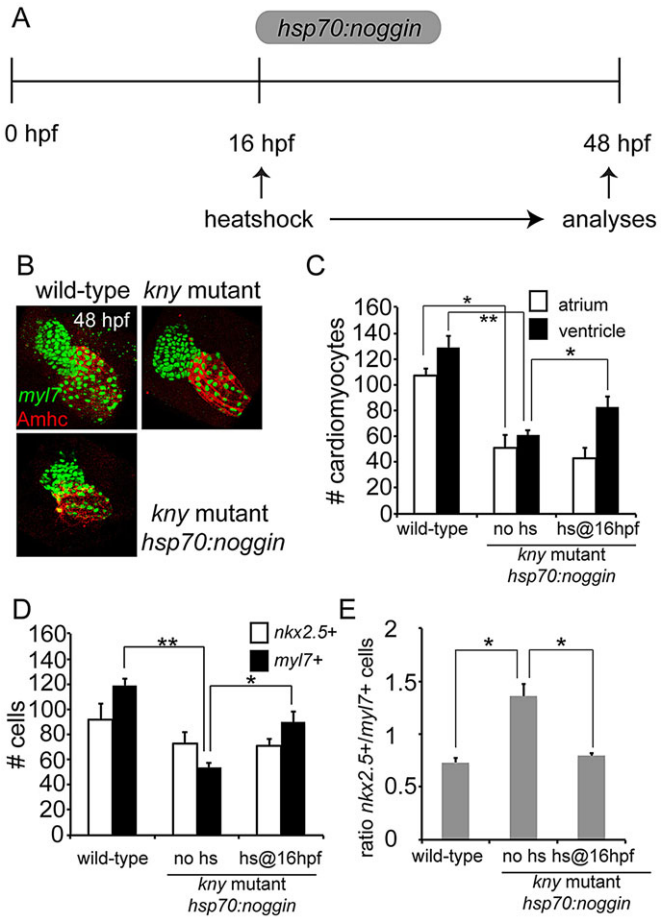

Fig. 5. Blocking Bmp signaling in *kny/gpc4* mutants restores cardiomyocyte differentiation. (A) *Tg(hsp70:noggin3)* embryos were heat-shocked at 16 hpf and analyzed at 48 hpf. (B) Reconstruction of confocal images of WT, *kny/gpc4* mutant and *kny/gpc4* mutant with *Tg(hsp70:noggin3)*, heat-shocked at 16 hpf. Embryos were stained for myl7:dsRed (false-colored in green) and Amhc (red). (C) Quantification of cardiomyocytes in ventricle and atrium of embryos shown in B (*n*=3 for each group). (D) Quantifications of *nkx2.5*$^{+}$ and *myl7*$^{+}$ cells in the ventricles of wild-type siblings, *kny/gpc4* mutants and *kny/gpc4* mutants after Noggin3 induction. (E) Ratio of *nkx2.5*$^{+}$/*myl7*$^{+}$ ventricular cells in wild-type siblings, *kny/gpc4* mutants and *kny/gpc4* mutants after Noggin3 induction. Results are represented as mean±s.e.m. **P*≤0.05, ***P*≤0.01 (paired *t*-test).

Development (2015) 142, 1767-1776 doi:10.1242/dev.113894

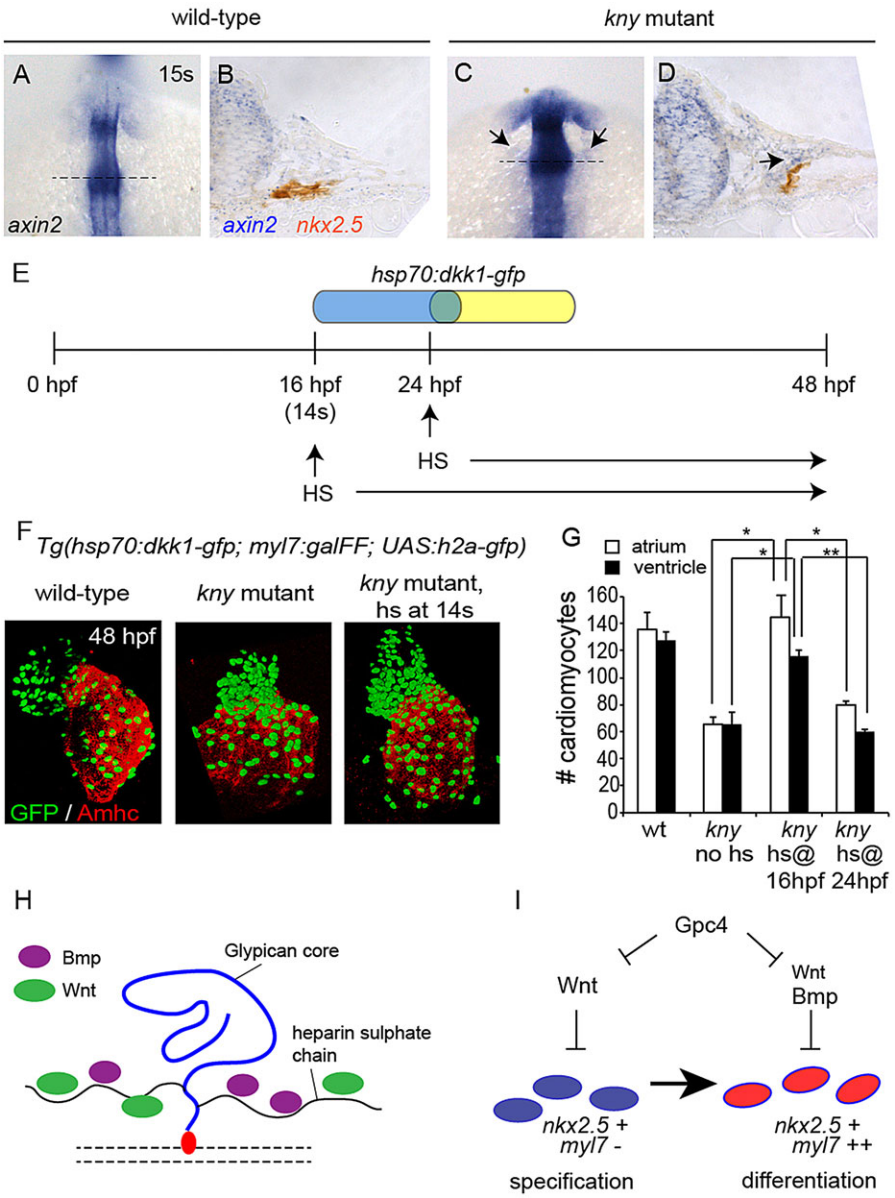

Fig. 6. Enhanced canonical Wnt signaling is responsible for reduced cardiomyocyte numbers in *kny*/*gpc4* mutants. (A-D) *In situ* hybridization for *axin2* at the 15-somite stage. Dorsal views (A,C) of WT (A,B) and *kny*/*gpc4* mutant (C,D). (B,D) Cross-sections through embryos stained for *axin2* (blue) and *nkx2.5* (orange) of WT (B) and *kny*/*gpc4* mutant (C). Arrows indicate ectopic *axin2* signal in anterior LPM. Dashed lines in A and C indicate location of the sections shown in B and D, respectively. (E) Timeline of rescue experiments with *Tg(hsp70:dkk1-gfp, myl7:galFF/UAS:h2a-gfp)*. HS, heat shock; 14s, 14-somite. (F) Confocal image reconstruction of wild-type or *kny*/*gpc4* mutant embryos with or without heat shock at 48 hpf, stained for GFP (green) and Amhc (red). (G) Quantification of cardiomyocytes in corresponding embryos (n=3). Results are represented as mean±s.e.m. *$P \leq 0.05$, **$P \leq 0.01$. (H) Schematic of GPI-anchored Glypican4 protein with heparin sulphate chains that can sequester growth factors, such as Wnt and Bmp, in the ECM. (I) Model summarizing the major findings of this work.

mutants displayed reduced looping and an enlarged atrial-ventricular canal, indicating that Glypican4 has other functions during heart development independent of canonical Wnt signaling. Besides the canonical Wnt pathway, Glypican4 also affects non-canonical Wnt signaling (Topczewski et al., 2001). Canonical and non-canonical Wnt signaling pathways can be simultaneously controlled by Syndecan-4, which inhibits canonical Wnt signaling through interaction with LRP6 and R-spondin 3 and activates the non-canonical Wnt pathway (Ohkawara et al., 2011; Astudillo et al., 2014). The importance of non-canonical Wnt signaling for cardiac development has been shown in numerous studies (Phillips et al., 2005; Schleiffarth et al., 2007; Zhou et al., 2007; Ramsbottom et al., 2014). Whether Glypican4 also affects non-canonical Wnt signaling in the anterior LPM is not addressed here.

Various studies have linked genetic alterations in glypican-coding genes with congenital heart defects. Heart defects in SGBS patients are very diverse and include defects of the outflow tract (transposition of the great arteries, pulmonary artery stenosis, aortic stenosis and patent ductus arteriosus) (Lin et al., 1999). The outflow tract derives from the SHF and defects in SHF differentiation lead to severe congenital outflow tract defects (Goddeeris et al., 2007). Nucleotide polymorphisms in *GPC5* have been brought into correlation with the occurrence of TOF (Quelin et al., 2009; Cordell et al., 2013). TOF patients display defects in SHF-derived structures (pulmonary stenosis, overriding aorta, ventricular septal defects) [reviewed by Page (1986)]. Together with our results presented here, this suggests that glypicans also have an important role in attenuating BMP and Wnt signaling to regulate cardiac outflow tract development in the anterior LPM of human embryos.

MATERIALS AND METHODS

All animal experiments were conducted under the guidelines of the animal welfare committee of the Royal Netherlands Academy of Arts and Sciences (KNAW).

Generation of transgenic lines

Tg(myl7:galFF; UAS:h2a-gfp)

The *I-SceI-myl7:galFF-SV40* construct was obtained by *Cla*I-*Xba*I cohesive-end cloning of the *galFF* sequence from *pT2KhspGFF*

Development (2015) 142, 1767-1776 doi:10.1242/dev.113894

(Asakawa and Kawakami, 2008) into I-*Sce*I-myl7-SV40 (a kind gift from S. Abdelilah-Seyfried, University of Potsdam, Germany), containing about 900 bp of the *myl7* promoter. Plasmid DNA was injected at 20 ng/µl in the presence of 0.75U I-*Sce*I meganuclease (New England Biolabs) into *Tg (UAS:rfp)* embryos (Asakawa and Kawakami, 2008). Healthy embryos displaying robust *myl7*-specific RFP fluorescence were grown to adulthood and screened for germline transmission, resulting in establishment of the *Tg(myl7:galFF/UAS:rfp)* transgenic line.

The *Tg(myl7:galFF/UAS:h2a-gfp)* line was generated by injecting plasmid plm262 at 20 ng/µl, a *h2a-gfp* in-frame version derived from plm74 (Koole and Tijsterman, 2014), in the presence of 25 ng/µl *tol2* mRNA into *Tg(myl7:galFF/UAS:rfp)* embryos. Healthy embryos displaying robust *myl7*-specific *h2a-gfp* fluorescence were grown to adulthood, resulting in establishment of the *Tg(myl7:galFF/UAS:h2A-gfp)* transgenic line.

Tg(nkx2.5BAC:galFF)

Recombineering of BAC clone DKEY-9I15 was performed following the manufacturer's protocol with minor modifications, as described in Bussmann and Schulte-Merker (2011). Primers used were *nkx2.5_Gal4FF_F*: 5′-CATAGGTACCTCTGATAAATCCCAACCGGATTATCCAAGTGG-ACCATCATACCATGAAGCTACTGTCTTCTATCG-AAC-3′ and *nkx2.5_KanR_R*: 5′-ATGTCCCGCACTGAGAAAGGAGTGGAAGTCATTTGG CTAGAGAACATTGCTCAGAAGAACTCGTCAAGA-AGGCG-3′.

BAC DNA was injected at 130 ng/µl in the presence of 25 ng/µl *tol2* mRNA into *Tg(UAS:gfp)* embryos (Asakawa and Kawakami, 2008). Healthy embryos displaying robust *nkx2.5*-specific fluorescence were grown to adulthood and screened for germline transmission, resulting in the establishment of the *Tg(nkx2.5BAC:galFF/UAS:gfp)* line. Subsequent outcross to *Tg(myl7:galFF/UAS:h2a-gfp)* carriers and selection of embryos with nuclear-specific GFP fluorescence in the *nkx2.5* expression domain resulted in the establishment of the *Tg(nkx2.5BAC:galFF/UAS:h2a-gfp)* transgenic line.

Zebrafish lines

In this study, the following zebrafish lines were used: *kny/gpc4* mutants that carried the *kny*^{fr6} allele (Topczewski et al., 2001). *Tg(myl7:EGFP)twu26* (Huang et al., 2003), hereafter referred to as *Tg(myl7:gfp)*, *Tg(nkx2.5:galFF/UAS:h2a-gfp)* as described above, *Tg(myl7:galFF, UAS:Kaede)* and *Tg(myl7:nlsKikGR)*^{hsc6} (Lazic and Scott, 2011), hereafter referred to as *Tg(myl:nlsKikGR)*, *Tg(hsp70:dkk1-gfp)* (Stoick-Cooper et al., 2007), *Tg(-5.1myl7:nDsRed2)*^{f2} (Mably et al., 2003), referred to as [*(Tg(myl7:dsred)*], *Tg(hsp70:wnt8a-gfp)* (Weidinger et al., 2005), *Tg(Bre:GFP)*^{p77} (Alexander et al., 2011), *Tg(bre:dmKO2)* fish (Collery and Link, 2011) and *Tg(hsp70I:Nog3)*^{fr14} (Chocron et al., 2007).

Microinjections

Wild-type embryos and *kny/gpc4* mutants were injected with 5 ng/µl of *kny/gpc4* mRNA into the yolk at the one-cell stage. Embryos were grown until 48 hpf and genotyped for the *kny/gpc4* mutation.

Acridine Orange staining

Embryos were incubated with a 2 µg/ml Acridine Orange solution in E3 medium for 45 min in the dark, rinsed three times in E3 medium and photographed live.

In situ hybridization

In situ hybridizations were carried out as described in Thisse and Thisse (2008). For double *in situ* hybridizations, the antibody was removed by washing embryos in 0.1 M glycin/HCl supplemented with 0.1% Tween, and afterwards in PBST. Embryos were incubated with anti-fluorescein antibody (Roche, 11426320001; 1:100) overnight. Following extensive washing with PBST and TBST, embryos were subjected to 2,4-iodophenyl-3-4-nitrophenyl-5-phenyl-tetrazolium chloride (INT) with BCIP (Roche), diluted in TBST until staining had developed. The embryos were fixed overnight in 4% PFA. Embryos were washed in PBST and mounted in glycerol before imaging. Riboprobes were transcribed from linearized template in the presence of digoxigenin- or fluorescein-11-UTP.

Cell counts

Cells were counted by using the *Tg(myl7:galFF/UAS:h2a-gfp)*, the *Tg(-5.1myl7:nDsRed2)*^{f2} (Mably et al., 2003) or the *Tg(nkx2.5BAC:galFF/UAS:h2a-gfp)* lines. Embryos were stained with anti-DsRed antibody (Clontech, 632496; 1:200) or anti-GFP antibody (rabbit anti-GFP, Torrey Pines Biolabs, TP401; 1:200; or anti-chicken GFP, Abcam, ab13970; 1:200) and anti-Myh6 antibody (S46 from the Hybridoma bank, 1:200). To count *nkx2.5*$^{+}$ cells expressing *gfp* in *Tg(hsp70:wnt8a-gfp)* fish, embryos were counterstained with DAPI after the antibody staining. The nuclear-specific DAPI staining was used to facilitate the counting of the *nkx2.5*$^{+}$ cells. Images were acquired by confocal microscopy. Three-dimensional (3D) reconstruction and cell counting were performed using Volocity software. Each cell-counting experiment was carried out on at least three biological repeats.

RT-qPCR

Total RNA was extracted from wild-type and *kny/gpc4* mutant embryos. cDNA was generated using the RTIII First Strand kit (Invitrogen). Quantitative PCRs were performed using SYBR Green (BioRad) in a BioRad MyIQ PCR machine. Gene expression levels were normalized to *gapdh* and *ef1a* levels and the ratio between wild-type and *kny/gpc4* mutant expression levels was calculated. Three biological repeats were used for each genotype and reactions were performed in triplicates. Primers used in this study were *nkx2.5*_F set 1: 5′-ACCTACAACACCTACCCTGCG-3′ and *nkx2.5*_R set 1: 5′-ACTGTGAAGGTTGGATGCTGGACA-3′ for qPCRs at 48 hpf and for the first biological experiment at 10 somite stage. For the second and third biological repeats at 10 somite stage, the following set was used: *nkx2.5*_F set 2: 5′-CAACACCTACCCTGCGTTTA-3′, *nkx2.5*_R set 2: 5′-GTTGGACTGTGAAGGTTGGA-3′, *gata4*_F: 5′-TCTCGCCATGAA GAAAGAGGG-3′, *gata4*_R: 5′-TGTGTGTGTAGAGCTGGTGTG-3′, *hand2*_F: 5′-CCAGTCGCTGTCATGAAGAA-3′, *hand2*_R: 5′-GTAC GAAGGTGCCATGGTATAG-3′, *cmlc2*_F: 5′-CTGTCTTCCTCACCCT CTTTG-3′ and *cmlc2*_R: 5′-TGACAACTCCTGTGGCATTAG-3′.

Photoconversion

Photoconversion of Kaede or nlsKikGR fluorescence from green to red was achieved by exposing transgenic embryos to a 405 nm laser, using a confocal microscope (Leica, TCS SPE) that allowed measuring the development of red fluorescence. Exposure was stopped when the red fluorescence had reached a maximum peak. Images were acquired by confocal microscopy. 3D reconstruction and cell counting were performed using Volocity software. The cell counting was performed on three biological repeats.

Histology

Vibratome sections were used to visualize *bre:gfp*$^{+}$ cells. Embryos were embedded in 3% agarose and 1% gelatin in PBS. Sections (50 µm) were stained overnight with primary antibody and secondary antibody overnight. Agarose slices were counterstained for 1 h with DAPI (Invitrogen, 1:2500). Antibody against tropomyosin (Sigma, T9283; 1:200) was used to visualize cardiac tissue. In order to visualize *axin2*-expressing cells, *Tg(nkx2.5:galFF/UAS:gfp)* embryos underwent *in situ* hybridization for *axin2* and subsequent staining with anti-*gfp* antibody (anti-rabbit GFP, Torrey Pines Biolabs, TP401; 1:200), followed by incubation with an anti-rabbit biotinylated secondary antibody (Vector Laboratories, BA-1000; 1:200). For sectioning, embryos were mounted in Technovit 8100 (Heraeus Kulzer) and sectioned at 7 µm.

Pixel intensity analysis

Mean gray values of GFP signal were measured within cardiac tissue, using histological cross-sections with the help of ImageJ (NIH). Mean gray values were measured in two wild-type and two mutant samples. The analysis was carried out on 14 cardiomyocytes in wild type and *kny/gpc4* mutants each. The amount of cells that displayed mean gray values above the 1.5-fold average value for wild-type cells were counted.

Development (2015) 142, 1767-1776 doi:10.1242/dev.113894

Heat-shock experiments

Embryos were heat-shocked by transferring them to E3 medium preheated to 37°C and incubation at 37°C for 30 min to induce the *hsp70:noggin* transgene, and for 45 min in case of *hsp70:wnt8a-gfp* and *hsp70:dkk1-gfp* transgenes. Cell counts were performed at 48 hpf, when the GFP signal from *hsp70:wnt8a-gfp* and *hsp70:dkk1-gfp* transgenes had ceased.

Acknowledgements

We would like to thank S. Chocron for technical assistance and E. Noël for critical reading of the manuscript.

Competing interests

The authors declare no competing or financial interests.

Author contributions

I.S. and J.B. conceived the research. F.T. generated the zebrafish transgenic lines. I.S. performed the experiments and analyzed the data together with J.B. I.S., F.T. and J.B. wrote and/or revised the manuscript.

Funding

I.S. was funded by the Deutsche Forschungsgemeinschaft (DFG) [grant: STR1225/1-1]. The work in J.B.'s laboratory was supported by the Netherlands Cardiovascular Research Initiative and the Dutch Heart Foundation [grant: Hustcare CVON 2011-2] and ZonMW [grant: 912.12.086].

Supplementary material

Supplementary material available online at
http://dev.biologists.org/lookup/suppl/doi:10.1242/dev.113894/-/DC1

References

Alexander, C., Zuniga, E., Blitz, I. L., Wada, N., Le Pabic, P., Javidan, Y., Zhang, T., Cho, K. W., Crump, J. G. and Schilling, T. F. (2011). Combinatorial roles for BMPs and Endothelin 1 in patterning the dorsal-ventral axis of the craniofacial skeleton. *Development* **138**, 5135-5146.

Andrée, B., Duprez, D., Vorbusch, B., Arnold, H.-H. and Brand, T. (1998). BMP-2 induces ectopic expression of cardiac lineage markers and interferes with somite formation in chicken embryos. *Mech. Dev.* **70**, 119-131.

Armengol, C., Cairo, S., Fabre, M. and Buendia, M. A. (2011). Wnt signaling and hepatocarcinogenesis: the hepatoblastoma model. *Int. J. Biochem. Cell Biol.* **43**, 265-270.

Asakawa, K. and Kawakami, K. (2008). Targeted gene expression by the Gal4-UAS system in zebrafish. *Dev. Growth Differ.* **50**, 391-399.

Astudillo, P., Carrasco, H. and Larrain, J. (2014). Syndecan-4 inhibits Wnt/beta-catenin signaling through regulation of low-density-lipoprotein receptor-related protein (LRP6) and R-spondin 3. *Int. J. Biochem. Cell Biol.* **46**, 103-112.

Avanesov, A., Honeyager, S. M., Malicki, J. and Blair, S. S. (2012). The role of glypicans in Wnt inhibitory factor-1 activity and the structural basis of Wif1's effects on Wnt and Hedgehog signaling. *PLoS Genet.* **8**, e1002503.

Bakkers, J. (2011). Zebrafish as a model to study cardiac development and human cardiac disease. *Cardiovasc. Res.* **91**, 279-288.

Belenkaya, T. Y., Han, C., Yan, D., Opoka, R. J., Khodoun, M., Liu, H. and Lin, X. (2004). Drosophila Dpp morphogen movement is independent of dynamin-mediated endocytosis but regulated by the glypican members of heparan sulfate proteoglycans. *Cell* **119**, 231-244.

Bertrand, N., Roux, M., Ryckebüsch, L., Niederreither, K., Dollé, P., Moon, A., Capecchi, M. and Zaffran, S. (2011). Hox genes define distinct progenitor sub-domains within the second heart field. *Dev. Biol.* **353**, 266-274.

Bussmann, J. and Schulte-Merker, S. (2011). Rapid BAC selection for tol2-mediated transgenesis in zebrafish. *Development* **138**, 4327-4332.

Cai, C.-L., Liang, X., Shi, Y., Chu, P.-H., Pfaff, S. L., Chen, J. and Evans, S. (2003). Isl1 identifies a cardiac progenitor population that proliferates prior to differentiation and contributes a majority of cells to the heart. *Dev. Cell* **5**, 877-889.

Cai, W., Albini, S., Wei, K., Willems, E., Guzzo, R. M., Tsuda, M., Giordani, L., Spiering, S., Kurian, L., Yeo, G. W. et al. (2013). Coordinate Nodal and BMP inhibition directs Baf60c-dependent cardiomyocyte commitment. *Genes Dev.* **27**, 2332-2344.

Caneparo, L., Huang, Y.-L., Staudt, N., Tada, M., Ahrendt, R., Kazanskaya, O., Niehrs, C. and Houart, C. (2007). Dickkopf-1 regulates gastrulation movements by coordinated modulation of Wnt/beta catenin and Wnt/PCP activities, through interaction with the Dally-like homolog Knypek. *Genes Dev.* **21**, 465-480.

Cano-Gauci, D. F., Song, H. H., Yang, H., McKerlie, C., Choo, B., Shi, W., Pullano, R., Piscione, T. D., Grisaru, S., Soon, S. et al. (1999). Glypican-3-deficient mice exhibit developmental overgrowth and some of the abnormalities typical of Simpson-Golabi-Behmel syndrome. *J. Cell Biol.* **146**, 255-264.

Chocron, S., Verhoeven, M. C., Rentzsch, F., Hammerschmidt, M. and Bakkers, J. (2007). Zebrafish Bmp4 regulates left-right asymmetry at two distinct developmental time points. *Dev. Biol.* **305**, 577-588.

Collery, R. F. and Link, B. A. (2011). Dynamic smad-mediated BMP signaling revealed through transgenic zebrafish. *Dev. Dyn.* **240**, 712-722.

Cordell, H. J., Topf, A., Mamasoula, C., Postma, A. V., Bentham, J., Zelenika, D., Heath, S., Blue, G., Cosgrove, C., Granados Riveron, J. et al. (2013). Genome-wide association study identifies loci on 12q24 and 13q32 associated with Tetralogy of Fallot. *Hum. Mol. Genet.* **22**, 1473-1481.

de Pater, E., Clijsters, L., Marques, S. R., Lin, Y.-F., Garavito-Aguilar, Z. V., Yelon, D. and Bakkers, J. (2009). Distinct phases of cardiomyocyte differentiation regulate growth of the zebrafish heart. *Development* **136**, 1633-1641.

de Pater, E., Ciampricotti, M., Priller, F., Veerkamp, J., Strate, I., Smith, K., Lagendijk, A. K., Schilling, T. F., Herzog, W., Abdelilah-Seyfried, S. et al. (2012). Bmp signaling exerts opposite effects on cardiac differentiation. *Circ. Res.* **110**, 578-587.

Desbordes, S. C. and Sanson, B. (2003). The glypican Dally-like is required for Hedgehog signalling in the embryonic epidermis of Drosophila. *Development* **130**, 6245-6255.

Dohn, T. E. and Waxman, J. S. (2012). Distinct phases of Wnt/beta-catenin signaling direct cardiomyocyte formation in zebrafish. *Dev. Biol.* **361**, 364-376.

Fico, A., Maina, F. and Dono, R. (2011). Fine-tuning of cell signaling by glypicans. *Cell. Mol. Life Sci.* **68**, 923-929.

Fujise, M., Takeo, S., Kamimura, K., Matsuo, T., Aigaki, T., Izumi, S. and Nakato, H. (2003). Dally regulates Dpp morphogen gradient formation in the Drosophila wing. *Development* **130**, 1515-1522.

Galli, D., Dominguez, J. N., Zaffran, S., Munk, A., Brown, N. A. and Buckingham, M. E. (2008). Atrial myocardium derives from the posterior region of the second heart field, which acquires left-right identity as Pitx2c is expressed. *Development* **135**, 1157-1167.

Goddeeris, M. M., Schwartz, R., Klingensmith, J. and Meyers, E. N. (2007). Independent requirements for Hedgehog signaling by both the anterior heart field and neural crest cells for outflow tract development. *Development* **134**, 1593-1604.

Golabi, M., Leung, A. and Lopez, C. (1993). Simpson-Golabi-Behmel syndrome type 1. In *GeneReviews(R)* (ed. R. A. Pagon, M. P. Adam, T. D. Bird, C. R. Dolan, C. T. Fong, R. J. H. Smith and K. Stephens). University of Washington, Seattle, WA.

Guner-Ataman, B., Paffett-Lugassy, N., Adams, M. S., Nevis, K. R., Jahangiri, L., Obregon, P., Kikuchi, K., Poss, K. D., Burns, C. E. and Burns, C. G. (2013). Zebrafish second heart field development relies on progenitor specification in anterior lateral plate mesoderm and nkx2.5 function. *Development* **140**, 1353-1363.

Hami, D., Grimes, A. C., Tsai, H.-J. and Kirby, M. L. (2011). Zebrafish cardiac development requires a conserved secondary heart field. *Development* **138**, 2389-2398.

Han, C., Yan, D., Belenkaya, T. Y. and Lin, X. (2005). Drosophila glypicans Dally and Dally-like shape the extracellular Wingless morphogen gradient in the wing disc. *Development* **132**, 667-679.

Hao, J., Daleo, M. A., Murphy, C. K., Yu, P. B., Ho, J. N., Hu, J., Peterson, R. T., Hatzopoulos, A. K. and Hong, C. C. (2008). Dorsomorphin, a selective small molecule inhibitor of BMP signaling, promotes cardiomyogenesis in embryonic stem cells. *PLoS ONE* **3**, e2904.

Hinits, Y., Pan, L., Walker, C., Dowd, J., Moens, C. B. and Hughes, S. M. (2012). Zebrafish Mef2ca and Mef2cb are essential for both first and second heart field cardiomyocyte differentiation. *Dev. Biol.* **369**, 199-210.

Honecker, F., Kersemaekers, A.-M., Molier, M., van Weeren, P. C., Stoop, H., de Krijger, R. R., Wolffenbuttel, K. P., Oosterhuis, W., Bokemeyer, C. and Looijenga, L. H. J. (2004). Involvement of E-cadherin and beta-catenin in germ cell tumours and in normal male fetal germ cell development. *J. Pathol.* **204**, 167-174.

Huang, C.-J., Tu, C.-T., Hsiao, C.-D., Hsieh, F.-J. and Tsai, H.-J. (2003). Germ-line transmission of a myocardium-specific GFP transgene reveals critical regulatory elements in the cardiac myosin light chain 2 promoter of zebrafish. *Dev. Dyn.* **228**, 30-40.

Hutson, M. R. and Kirby, M. L. (2007). Model systems for the study of heart development and disease: cardiac neural crest and conotruncal malformations. *Semin. Cell Dev. Biol.* **18**, 101-110.

Jackson, S. M., Nakato, H., Sugiura, M., Jannuzi, A., Oakes, R., Kaluza, V., Golden, C. and Selleck, S. B. (1997). dally, a Drosophila glypican, controls cellular responses to the TGF-beta-related morphogen, Dpp. *Development* **124**, 4113-4120.

Kelly, R. G. (2012). The second heart field. *Curr. Top. Dev. Biol.* **100**, 33-65.

Kelly, R. G., Brown, N. A. and Buckingham, M. E. (2001). The arterial pole of the mouse heart forms from Fgf10-expressing cells in pharyngeal mesoderm. *Dev. Cell* **1**, 435-440.

Klaus, A., Muller, M., Schulz, H., Saga, Y., Martin, J. F. and Birchmeier, W. (2012). Wnt/beta-catenin and Bmp signals control distinct sets of transcription factors in cardiac progenitor cells. *Proc. Natl. Acad. Sci. USA* **109**, 10921-10926.

Koole, W. and Tijsterman, M. (2014). Mosaic analysis and tumor induction in zebrafish by microsatellite instability-mediated stochastic gene expression. *Dis. Model. Mech.* **7**, 929-936.
Lapunzina, P. (2005). Risk of tumorigenesis in overgrowth syndromes: a comprehensive review. *Am. J. Med. Genet. C Semin. Med. Genet.* **137C**, 53-71.
Lazic, S. and Scott, I. C. (2011). Mef2cb regulates late myocardial cell addition from a second heart field-like population of progenitors in zebrafish. *Dev. Biol.* **354**, 123-133.
Li, J., Kleeff, J., Kayed, H., Felix, K., Penzel, R., Büchler, M. W., Korc, M. and Friess, H. (2004). Glypican-1 antisense transfection modulates TGF-beta-dependent signaling in Colo-357 pancreatic cancer cells. *Biochem. Biophys. Res. Commun.* **320**, 1148-1155.
Lin, X. and Perrimon, N. (1999). Dally cooperates with Drosophila Frizzled 2 to transduce Wingless signalling. *Nature* **400**, 281-284.
Lin, A. E., Neri, G., Hughes-Benzie, R. and Weksberg, R. (1999). Cardiac anomalies in the Simpson-Golabi-Behmel syndrome. *Am. J. Med. Genet.* **83**, 378-381.
Liu, X., Mazanek, P., Dam, V., Wang, Q., Zhao, H., Guo, R., Jagannathan, J., Cnaan, A., Maris, J. M. and Hogarty, M. D. (2008). Deregulated Wnt/beta-catenin program in high-risk neuroblastomas without MYCN amplification. *Oncogene* **27**, 1478-1488.
Mably, J. D., Mohideen, M. A., Burns, C. G., Chen, J.-N. and Fishman, M. C. (2003). heart of glass regulates the concentric growth of the heart in zebrafish. *Curr. Biol.* **13**, 2138-2147.
Manisastry, S. M., Han, M. and Linask, K. K. (2006). Early temporal-specific responses and differential sensitivity to lithium and Wnt-3A exposure during heart development. *Dev. Dyn.* **235**, 2160-2174.
Mateos, M. E., Beyer, K., López-Laso, E., Siles, J. L., Pérez-Navero, J. L., Peña, M. J., Guzmán, J. and Matas, J. (2013). Simpson-Golabi-Behmel syndrome type 1 and hepatoblastoma in a patient with a novel exon 2-4 duplication of the GPC 3 gene. *Am. J. Med. Genet. A* **161**, 1091-1095.
Matsui, H., Ikeda, K., Nakatani, K., Sakabe, M., Yamagishi, T., Nakanishi, T. and Nakajima, Y. (2005). Induction of initial cardiomyocyte alpha-actin–smooth muscle alpha-actin–in cultured avian pregastrula epiblast: a role for nodal and BMP antagonist. *Dev. Dyn.* **233**, 1419-1429.
Mjaatvedt, C. H., Nakaoka, T., Moreno-Rodriguez, R., Norris, R. A., Kern, M. J., Eisenberg, C. A., Turner, D. and Markwald, R. R. (2001). The outflow tract of the heart is recruited from a novel heart-forming field. *Dev. Biol.* **238**, 97-109.
Nakato, H., Futch, T. A. and Selleck, S. B. (1995). The division abnormally delayed (dally) gene: a putative integral membrane proteoglycan required for cell division patterning during postembryonic development of the nervous system in Drosophila. *Development* **121**, 3687-3702.
Ng, A., Wong, M., Viviano, B., Erlich, J. M., Alba, G., Pflederer, C., Jay, P. Y. and Saunders, S. (2009). Loss of glypican-3 function causes growth factor-dependent defects in cardiac and coronary vascular development. *Dev. Biol.* **335**, 208-215.
Ohkawara, B., Glinka, A. and Niehrs, C. (2011). Rspo3 binds syndecan 4 and induces Wnt/PCP signaling via clathrin-mediated endocytosis to promote morphogenesis. *Dev. Cell* **20**, 303-314.
Page, G. G. (1986). Tetralogy of Fallot. *Heart Lung* **15**, 390-401.
Paine-Saunders, S., Viviano, B. L., Zupicich, J., Skarnes, W. C. and Saunders, S. (2000). glypican-3 controls cellular responses to Bmp4 in limb patterning and skeletal development. *Dev. Biol.* **225**, 179-187.
Phillips, H. M., Murdoch, J. N., Chaudhry, B., Copp, A. J. and Henderson, D. J. (2005). Vangl2 acts via RhoA signaling to regulate polarized cell movements during development of the proximal outflow tract. *Circ. Res.* **96**, 292-299.
Quélin, C., Bendavid, C., Dubourg, C., de la Rochebrochard, C., Lucas, J., Henry, C., Jaillard, S., Loget, P., Loeuillet, L., Lacombe, D. et al. (2009). Twelve new patients with 13q deletion syndrome: genotype-phenotype analyses in progress. *Eur. J. Med. Genet.* **52**, 41-46.
Ramsbottom, S. A., Sharma, V., Rhee, H. J., Eley, L., Phillips, H. M., Rigby, H. F., Dean, C., Chaudhry, B. and Henderson, D. J. (2014). Vangl2-regulated polarisation of second heart field-derived cells is required for outflow tract lengthening during cardiac development. *PLoS Genet.* **10**, e1004871.
Rodríguez-Criado, G., Magano, L., Segovia, M., Gurrieri, F., Neri, G., González-Meneses, A., Gómez de Terreros, I., Valdéz, R., Gracia, R. and Lapunzina, P. (2005). Clinical and molecular studies on two further families with Simpson-Golabi-Behmel syndrome. *Am. J. Med. Genet. A* **138A**, 272-277.
Sakane, H., Yamamoto, H., Matsumoto, S., Sato, A. and Kikuchi, A. (2012). Localization of glypican-4 in different membrane microdomains is involved in the regulation of Wnt signaling. *J. Cell Sci.* **125**, 449-460.
Schlange, T., Andrée, B., Arnold, H.-H. and Brand, T. (2000). BMP2 is required for early heart development during a distinct time period. *Mech. Dev.* **91**, 259-270.
Schleiffarth, J. R., Person, A. D., Martinsen, B. J., Sukovich, D. J., Neumann, A., Baker, C. V. H., Lohr, J. L., Cornfield, D. N., Ekker, S. C. and Petryk, A. (2007). Wnt5a is required for cardiac outflow tract septation in mice. *Pediatr. Res.* **61**, 386-391.
Schoenebeck, J. J., Keegan, B. R. and Yelon, D. (2007). Vessel and blood specification override cardiac potential in anterior mesoderm. *Dev. Cell* **13**, 254-267.
Schultheiss, T. M., Burch, J. B. and Lassar, A. B. (1997). A role for bone morphogenetic proteins in the induction of cardiac myogenesis. *Genes Dev.* **11**, 451-462.
Solnica-Krezel, L., Stemple, D. L., Mountcastle-Shah, E., Rangini, Z., Neuhauss, S. C., Malicki, J., Schier, A. F., Stainier, D. Y., Zwartkruis, F., Abdelilah, S. et al. (1996). Mutations affecting cell fates and cellular rearrangements during gastrulation in zebrafish. *Development* **123**, 67-80.
Stoick-Cooper, C. L., Weidinger, G., Riehle, K. J., Hubbert, C., Major, M. B., Fausto, N. and Moon, R. T. (2007). Distinct Wnt signaling pathways have opposing roles in appendage regeneration. *Development* **134**, 479-489.
Taha, M. F., Valojerdi, M. R. and Mowla, S. J. (2007). Effect of bone morphogenetic protein-4 (BMP-4) on cardiomyocyte differentiation from mouse embryonic stem cell. *Int. J. Cardiol.* **120**, 92-101.
Thisse, C. and Thisse, B. (2008). High-resolution in situ hybridization to whole-mount zebrafish embryos. *Nat. Protoc.* **3**, 59-69.
Thomas, M., Enciso, V., Stratton, R., Shah, S., Winder, T., Tayeh, M. and Roeder, E. (2012). Metastatic medulloblastoma in an adolescent with Simpson-Golabi-Behmel syndrome. *Am. J. Med. Genet. A* **158A**, 2534-2536.
Topczewski, J., Sepich, D. S., Myers, D. C., Walker, C., Amores, A., Lele, Z., Hammerschmidt, M., Postlethwait, J. and Solnica-Krezel, L. (2001). The zebrafish glypican knypek controls cell polarity during gastrulation movements of convergent extension. *Dev. Cell* **1**, 251-264.
Tsuda, M., Kamimura, K., Nakato, H., Archer, M., Staatz, W., Fox, B., Humphrey, M., Olson, S., Futch, T., Kaluza, V. et al. (1999). The cell-surface proteoglycan Dally regulates Wingless signalling in Drosophila. *Nature* **400**, 276-280.
Verhoeven, M. C., Haase, C., Christoffels, V. M., Weidinger, G. and Bakkers, J. (2011). Wnt signaling regulates atrioventricular canal formation upstream of BMP and Tbx2. *Birth Defect. Res. A Clin. Mol. Teratol.* **91**, 435-440.
Verma, M. K. and Lenka, N. (2010). Temporal and contextual orchestration of cardiac fate by WNT-BMP synergy and threshold. *J. Cell. Mol. Med.* **14**, 2094-2108.
Vincent, S. D. and Buckingham, M. E. (2010). How to make a heart: the origin and regulation of cardiac progenitor cells. *Curr. Top. Dev. Biol.* **90**, 1-41.
Waldo, K. L., Kumiski, D. H., Wallis, K. T., Stadt, H. A., Hutson, M. R., Platt, D. H. and Kirby, M. L. (2001). Conotruncal myocardium arises from a secondary heart field. *Development* **128**, 3179-3188.
Waterson, J., Stockley, T. L., Segal, S. and Golabi, M. (2010). Novel duplication in glypican-4 as an apparent cause of Simpson-Golabi-Behmel syndrome. *Am. J. Med. Genet. A* **152A**, 3179-3181.
Weidinger, G., Thorpe, C. J., Wuennenberg-Stapleton, K., Ngai, J. and Moon, R. T. (2005). The Sp1-related transcription factors sp5 and sp5-like act downstream of Wnt/beta-catenin signaling in mesoderm and neuroectoderm patterning. *Curr. Biol.* **15**, 489-500.
Willems, E., Spiering, S., Davidovics, H., Lanier, M., Xia, Z., Dawson, M., Cashman, J. and Mercola, M. (2011). Small-molecule inhibitors of the Wnt pathway potently promote cardiomyocytes from human embryonic stem cell-derived mesoderm. *Circ. Res.* **109**, 360-364.
Williams, E. H., Pappano, W. N., Saunders, A. M., Kim, M.-S., Leahy, D. J. and Beachy, P. A. (2010). Dally-like core protein and its mammalian homologues mediate stimulatory and inhibitory effects on Hedgehog signal response. *Proc. Natl. Acad. Sci. USA* **107**, 5869-5874.
Xu, H., Morishima, M., Wylie, J. N., Schwartz, R. J., Bruneau, B. G., Lindsay, E. A. and Baldini, A. (2004). Tbx1 has a dual role in the morphogenesis of the cardiac outflow tract. *Development* **131**, 3217-3227.
Yuasa, S., Itabashi, Y., Koshimizu, U., Tanaka, T., Sugimura, K., Kinoshita, M., Hattori, F., Fukami, S.-i., Shimazaki, T., Okano, H. et al. (2005). Transient inhibition of BMP signaling by Noggin induces cardiomyocyte differentiation of mouse embryonic stem cells. *Nat. Biotechnol.* **23**, 607-611.
Zaffran, S. and Kelly, R. G. (2012). New developments in the second heart field. *Differentiation* **84**, 17-24.
Zhou, W., Lin, L., Majumdar, A., Li, X., Zhang, X., Liu, W., Etheridge, L., Shi, Y., Martin, J., Van de Ven, W. et al. (2007). Modulation of morphogenesis by noncanonical Wnt signaling requires ATF/CREB family-mediated transcriptional activation of TGFbeta2. *Nat. Genet.* **39**, 1225-1234.
Zhou, Y., Cashman, T. J., Nevis, K. R., Obregon, P., Carney, S. A., Liu, Y., Gu, A., Mosimann, C., Sondalle, S., Peterson, R. E. et al. (2011). Latent TGF-beta binding protein 3 identifies a second heart field in zebrafish. *Nature* **474**, 645-648.

Supplementary Figures

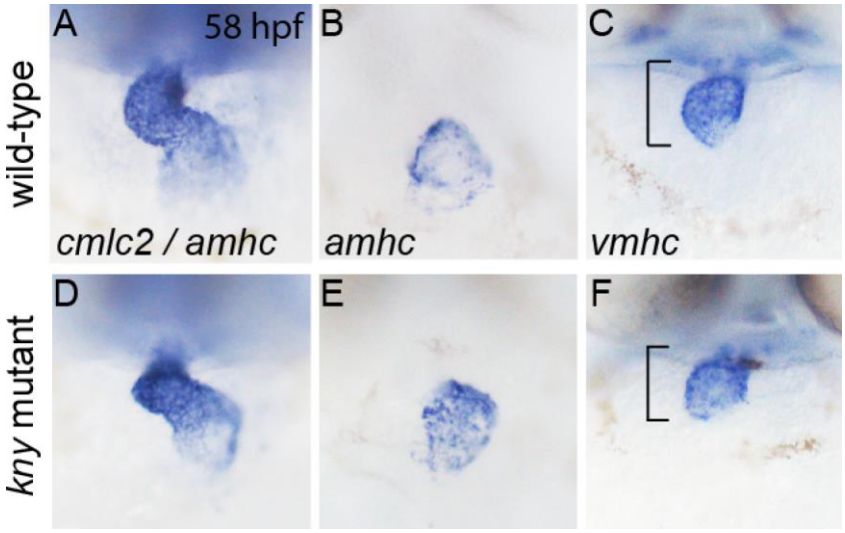

Figure S1, related to Figure 1: Reduced heart looping and reduced chamber sizes in *kny/gpc4* mutants. (A-F) Anterior view of *in situ* hybridized wild-type (A-C) and *kny/gpc4* mutant (D-F) at 58 hpf. *In situ* hybridization was carried out for *amhc/cmlc2* (A,D), *amhc* alone (B,E) and *vmhc* (C,F).

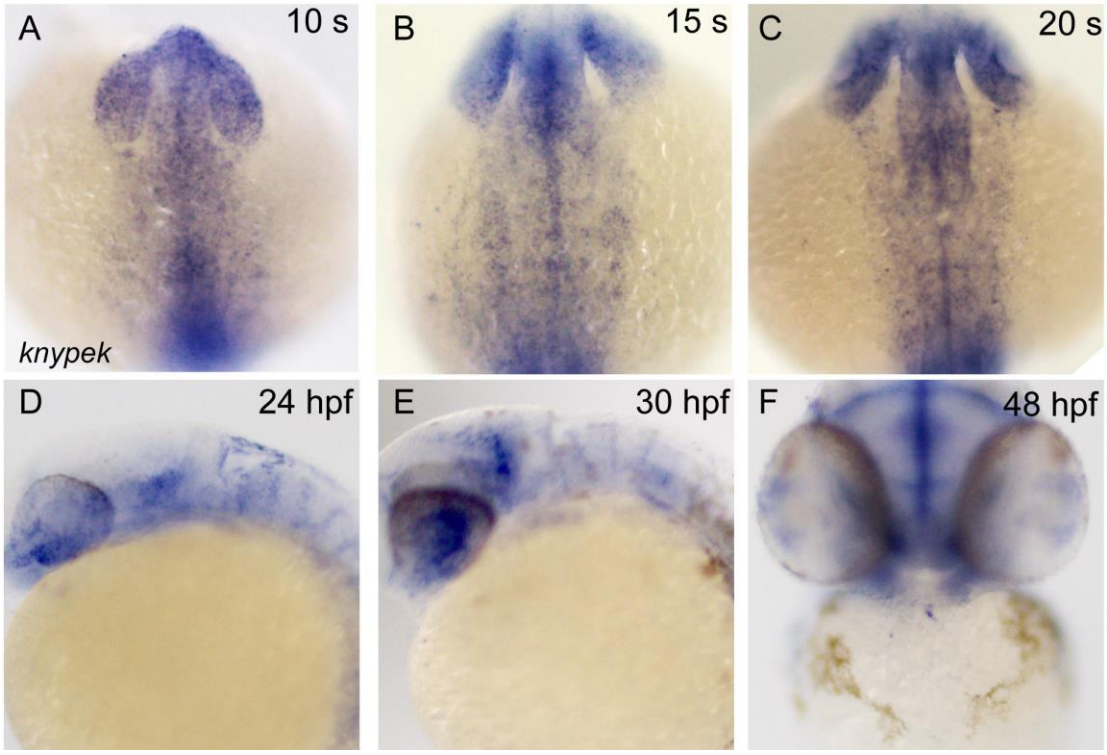

Figure S2, related to Figure 1: *Kny/gpc4* expression in wild-type embryos.

(A-C) Dorsal view of wild-type embryos at 10-somite, 15-somite and 20-somite stages, respectively. (D-F) Lateral view of wild-type embryos at 24, 30 and 48 hpf, respectively. *In situ* hybridization was performed for *kny/gpc4*.

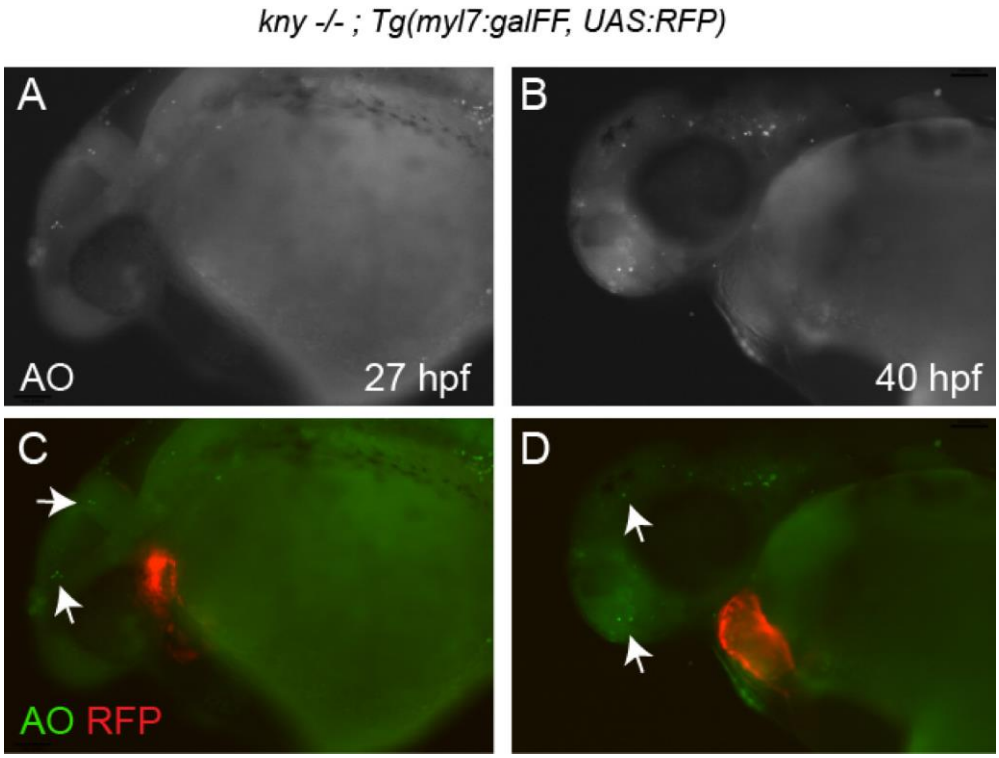

Figure S3, related to Figure 1: Acridine Orange staining of *kny/gpc4* mutants.

Live images of kny/gpc4 mutant embryos at 27 hpf (A,C) and 40 hpf (B,D) stained with Acridine Orange (AO) to visualize apoptotic cells (green). Arrows indicate apoptotic cells in brain region. No apoptotic cells were observed in the myocardium of *kny/gpc4* mutant hearts (red).

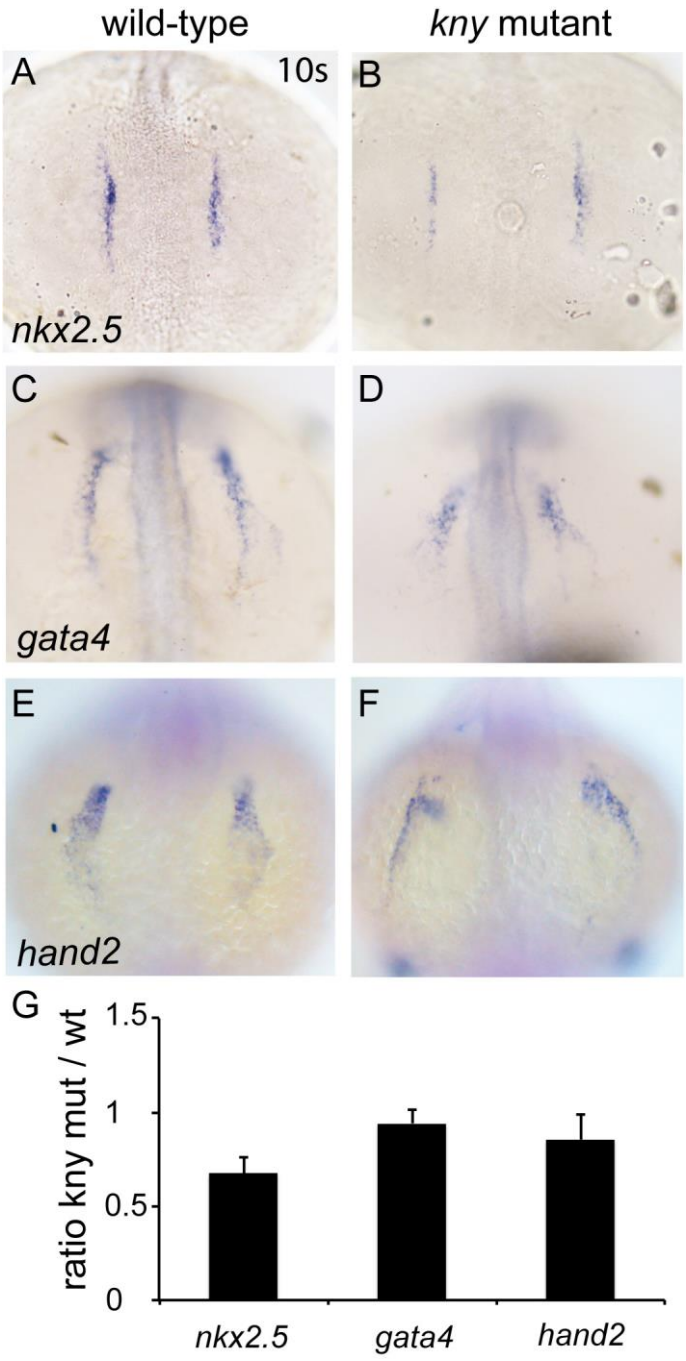

Figure S4, related to Figure 2: Cardiac specification in *kny/gpc4* mutants. (A-F) Dorsal view of wild-types (A,C,E) and *kny/gpc4* mutants (B,D,F) at 10-somite stage. *In situ* hybridization was carried out for *nkx2.5* (A and B), *gata4* (C and D) and *hand2* (E and F). (G) qPCR results of embryos from corresponding stages. Gene expression levels were normalized against *ef1a.* The *y*-axis represents the ratio of expression levels between *kny/gpc4* mutants and wild-type siblings (three biological repeats). Results are represented as mean±s.e.m.

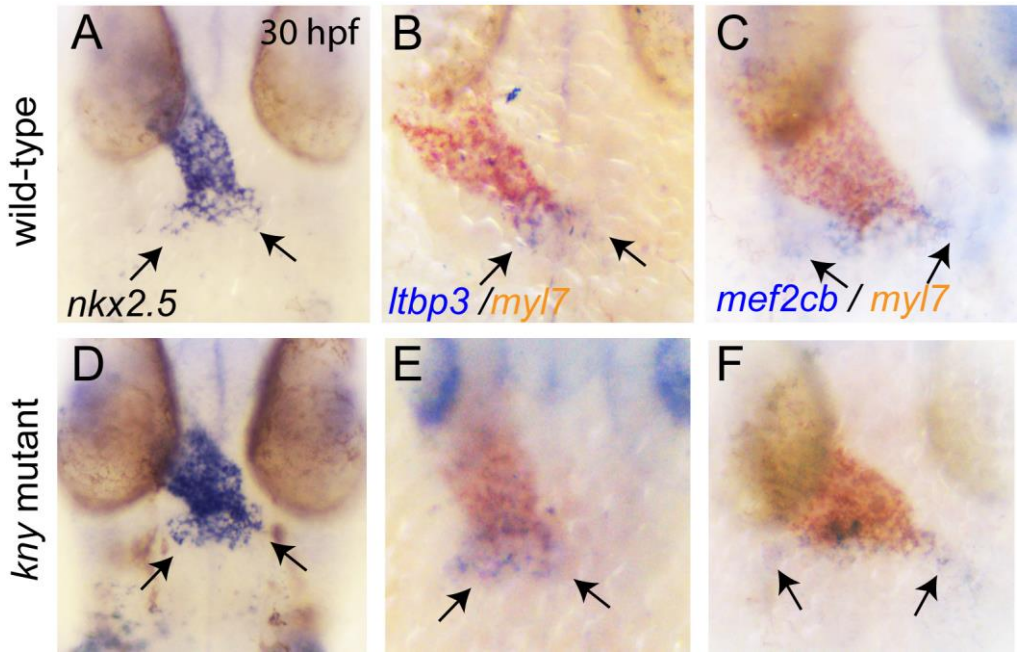

Figure S5, related to Figure 2: Specification of the SHF occurs in *kny/gpc4* mutants. (A-F) Dorsal view of wild-types (A-C) and *kny/gpc4* mutants (D-F) at 30 hpf. *In situ* hybridization was carried out for *nkx2.5* (A,D), *ltbp3* (blue) / *myl7* (orange) (B,E) and *mef2cb* (blue)/*myl7* (orange) (C,F). Arrows indicate staining in the SHF.

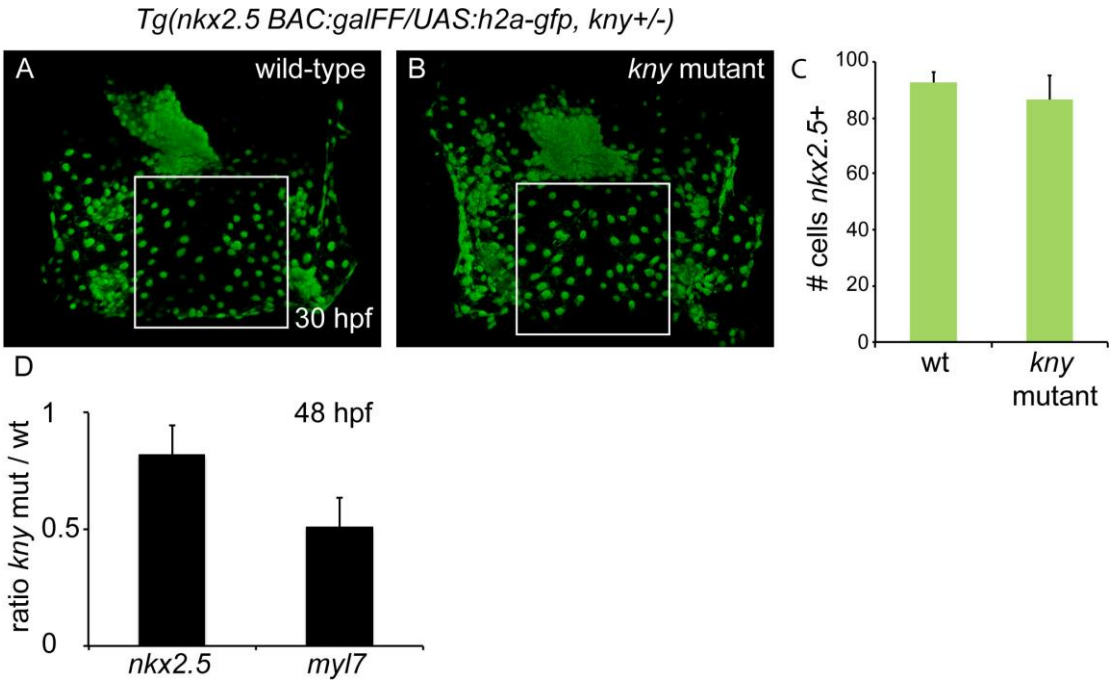

Figure S6, related to Figure 3: Nkx2.5+ cells in the anterior LPM of *kny/gpc4* mutants and wild-type siblings (A,B) Dorsal view of wild-type (A) and *kny/gpc4* mutant (B), expressing the *nkx2.5:galFF/UAS:h2a-gfp* transgene at 30 hpf. (C) Numbers of *nkx2.5*+ cells in boxed areas from (A,B). (D) qPCR results of *nkx2.5* and *myl7* expression levels at 48 hpf. Normalization against *ef1a*. The y-axis represents the ratio of expression level between *kny/gpc4* mutants and wild-type siblings (three biological repeats). Results are represented as mean±s.e.m.

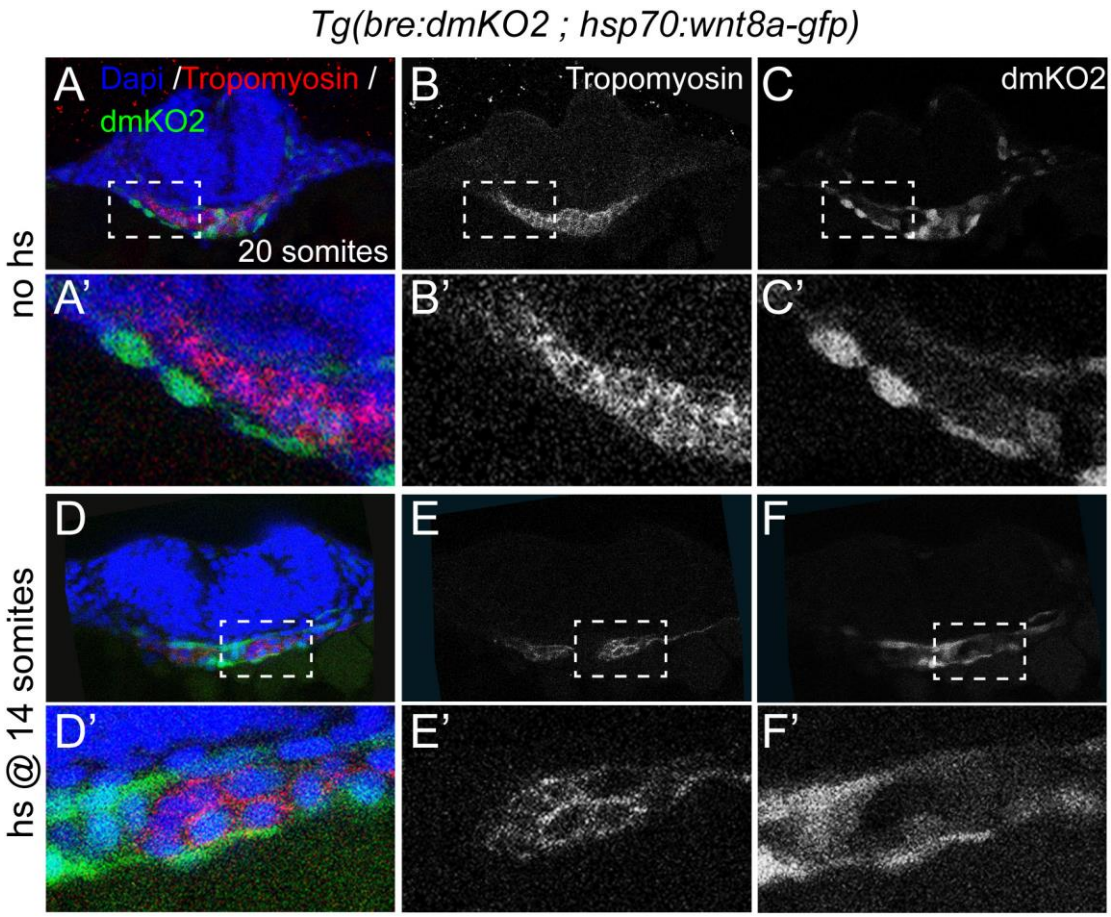

Figure S7, related to Figure 4: Ectopic Wnt8 expression does not induce *bre:dmKO2* activity. Cross-sections through anterior LPM of control (A-C') or heat-shocked (D-F') embryo of 20-somites with *Tg(bre:dmKO2 ; hsp70:wnt8a-gfp)*. Embryos in (D-F') were heat shocked at 16 hpf (14 somites). Cell nuclei are shown in blue (DAPI), cardiac tissue in red (tropomyosin) and Bmp activity in green (*bre:dmKO2* transgene). (A'-F') are magnifications of boxed areas in (A-F).

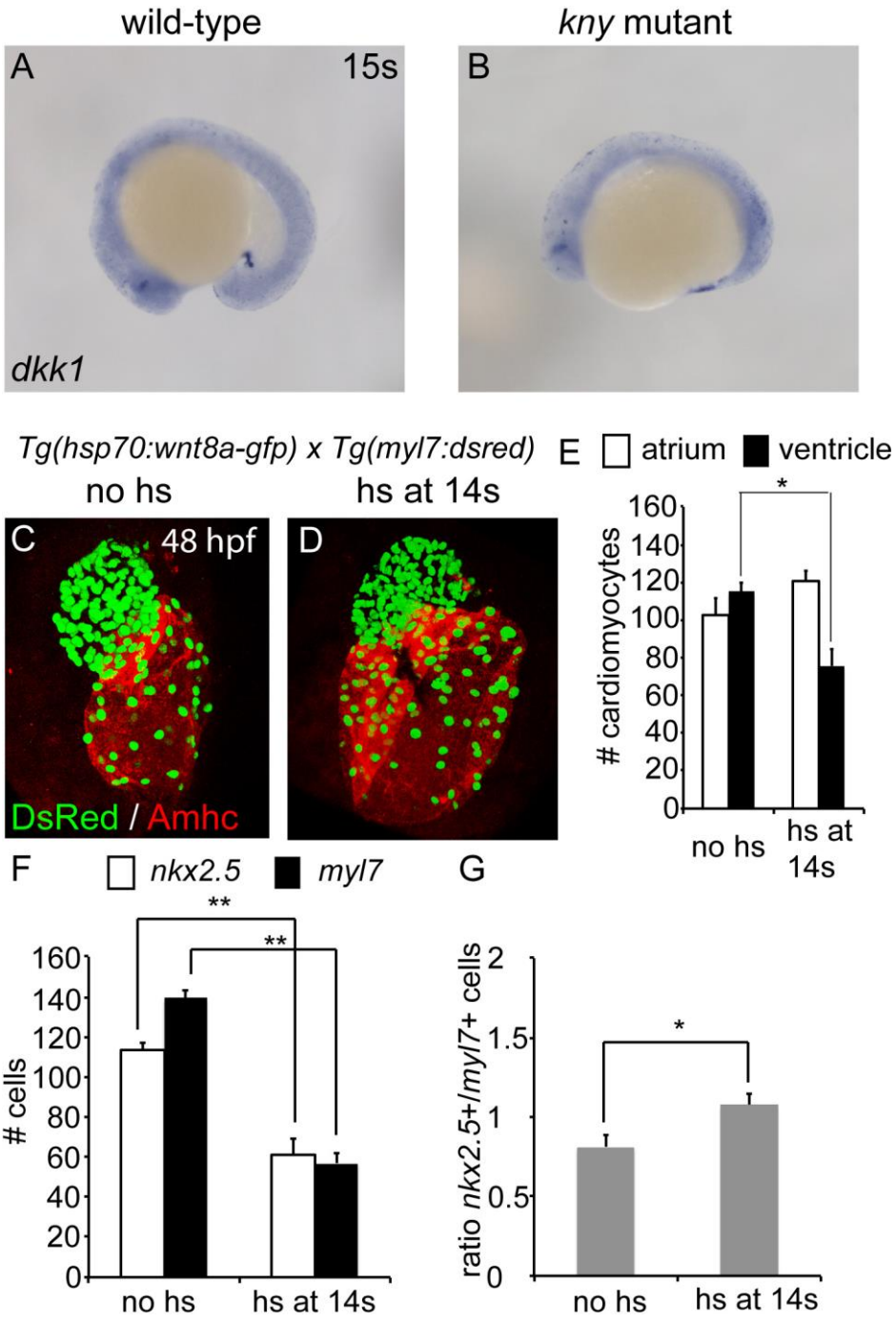

Figure S8, related to Figure 4: Elevation of canonical Wnt signaling after cardiac specification leads to a reduction of ventricular cardiomyocytes. (A,B) Lateral view of wild-type siblings and *kny/gpc4* mutants after in situ hybridization for *dkk1* at the 15 somite stage. (C,D) Hearts at 48 hpf of embryos derived from the *Tg(hsp70:wnt8a-gfp)* line crossed to *Tg(myl7:dsred),* stained for DsRed (false colored in green) and Amhc (red). (E)

Cardiomyocyte numbers of corresponding hearts (*n*=3). (F) Quantification of *nkx2.5+* and *myl7+* cells in the ventricles of embryos after *wnt8a* induction (n=3). (G) Ratio of *nkx2.5+/myl7+* cells in corresponding hearts after Wnt8 induction. Results are represented as mean ±s.e.m. Asterisks represents statistical significance according to a paired *t*-test: * $P<0.05$; ** $P<0.01$.